

**“STUDY OF SLOPE STABILITY USING GEOSYNTHETICS”**

A DISSERTATION  
SUBMITTED IN PARTIAL FULFILLMENT  
FOR REQUIREMENT OF THE DEGREE OF  
MASTER OF TECHNOLOGY  
IN  
**CIVIL ENGINEERING**  
**(Geotechnical Engineering)**

Submitted by  
**SHUBHAM SINGHAL**  
**(2K21/GTE/22)**

Under the supervision of  
**Prof. AMIT KUMAR SRIVASTAVA**



**CIVIL ENGINEERING DEPARTMENT**  
**DELHI TECHNOLOGICAL UNIVERSITY**  
Bawana Road, Delhi-110042

MAY-2023

DELHI TECHNOLOGICAL UNIVERSITY

(Formerly Delhi College of Engineering)

Bawana Road, Delhi-110042

**CANDIDATE'S DECLARATION**

I, **Shubham Singhal, 2K21/GTE/22**, student of M. Tech (Civil Engineering), hereby declare that the project dissertation titled “**Study of Slope Stability using Geosynthetics**” is submitted to the Department of Civil Engineering, Delhi Technological University, Delhi, by me in partial fulfillment of requirement for the award of degree of **Master of Technology (Geotechnical Engineering)**. This thesis is original work done by me and not obtained from any source without proper citation. This project work has not previously formed the basis for award of any degree, diploma, fellowship or other similar title or recognition.

Place: Delhi

**SHUBHAM SINGHAL**

**(2K21/GTE/22)**

Date: 31/05/2023

**DEPARTMENT OF CIVIL ENGINEERING**

**DELHI TECHNOLOGICAL UNIVERSITY**

(Formerly Delhi College of Engineering)

Bawana Road, Delhi-110042

**CERTIFICATE**

I hereby certify that project dissertation titled “**Study of Slope Stability using Geosynthetics**” submitted by **Shubham Singhal, 2K21/GTE/22**, Department of Civil Engineering, Delhi Technological University, Delhi, in partial fulfillment for the award of degree of Master of Technology, is a project work carried out by the student under my supervision. To the best of my knowledge, this work has not been submitted in part or full for any degree or diploma to this university or elsewhere.

Supervisor

**Prof. AMIT KUMAR SRIVASTAVA**

DEPARTMENT OF CIVIL ENGINEERING

Delhi Technological University,

Delhi-110042

## ABSTRACT

During the monsoons, significant precipitation falls upon the Shimla district of the Lesser Himalayas. During rainy seasons, slope failures produce landslides in the region. The Shimla district has a significant problem with landslides. More landslides and subsidence's have occurred in recent decades because of the construction of roads and buildings on top of a weak geological structure. A feasible option is to incorporate the geosynthetics into the slope in order to provide the drainage as well as reinforcement required to safeguard the stability of slope in the event of precipitation. In this paper, GeoStudio was used to investigate the impact of precipitation over the drainage factors & overall slope stability together with & without geosynthetics. This study examines the stability of a failing slope located in the Shimla region of Himachal Pradesh using numerical modelling before and after rainfalls of varying intensities, including max. rainfall, min. rainfall, & avg. rainfall. Before rainfall or monsoon, the factor of safety was higher than 1, showing a stable slope. For slopes with slope angles of  $37.65^\circ$  and  $42^\circ$ , the factor of safety at maximum rainfall was calculated to be 0.992 and 0.928, which is less than 1, indicating an unstable slope. Now the failed slopes were stabilised using geosynthetics in 3,4,5 and 6 layers. After using geosynthetics slope were stabilised and their factor of safety came out to be greater than 1.

**Keywords:** - Numerical Modelling, Slope stability, Geosynthetics, Critical Slip surfaces,

**Seepage**

## **ACKNOWLEDGEMENTS**

I express my deep gratitude and indebtedness to **Prof. Amit Kumar Srivastava**, Department of Civil Engineering, DTU, Delhi, for his guidance, and valuable feedback throughout this project work. His able knowledge and supervision with unswerving patience fathered my project work at every stage, for without his encouragement, the fulfilment of task would have been impossible and difficult.

I wish to express my gratitude towards our Head of Department, **Prof. V. K. Minocha**, Department of Civil Engineering, DTU, Delhi, for showing interest and providing help throughout the period of my project work.

I am genuinely appreciative of all my Friends for their support and suggestions during my work. Lastly, I would like to thank the Almighty GOD and my parents, whose committed and untiring efforts towards me have brought me at this stage of my life.

**SHUBHAM SINGHAL**

**(2K21/GTE/22)**

**Date: 31/05/2023**

# Table of Contents

CANDIDATE’S DECLARATION .....	ii
CERTIFICATE .....	iii
ABSTRACT.....	iv
ACKNOWLEDGEMENTS .....	v
List of Tables .....	viii
List of Figures .....	ix
CHAPTER 1 INTRODUCTION .....	1
1.1    General .....	1
1.2    Causes of Failure of slope .....	2
1.3    Effect of rainfall on the stability of slope.....	3
1.4    Overview of Slope/W of GeoStudio software.....	4
1.5    Different methods of analysis .....	4
1.5.1    Limit Equilibrium Method .....	4
1.5.2    Morgenstern Price method .....	4
1.5.3    Finite Element Method .....	5
1.6    Geosynthetics .....	5
1.7    Objectives of current study .....	6
CHAPTER 2 LITERATURE REVIEW .....	7
CHAPTER 3 STUDY LOCATION.....	14
3.1 Area of Study .....	14
3.2 Description of the Field of Study and properties of materials .....	14
3.3 Rainfall Characteristics .....	16
CHAPTER 4 METHODOLOGY .....	18
4.1 Experimental Studies .....	18
4.1.1 Particle Size Distribution Analysis .....	18
4.1.2 Determination of Specific Gravity .....	20
4.1.3 Atterberg Limits Test.....	20
4.1.4 Compaction Test .....	21
4.1.5 Direct Shear Test (DST) .....	21
4.2 Numerical Modelling .....	22
4.2.1 Seepage Analysis During Rainfall .....	22
4.2.2 Analysis of slope stability using SLOPE/W .....	24
CHAPTER 5 RESULTS AND DISCUSSIONS.....	26
5.1 Experimental Results .....	26
5.1.1 Particle Size Distribution Analysis .....	26

5.1.2 Specific Gravity Test .....	27
5.1.3 Atterberg Limits Test.....	27
5.1.4 Compaction Test .....	28
5.1.5 Direct Shear Test.....	29
5.2 Numerical Modelling .....	30
5.2.1 Without Geosynthetics.....	30
5.2.1.1 Before Rainfall.....	30
5.2.1.2 After Rainfall .....	33
5.2.2 With Geosynthetics .....	39
5.2.2.1 After Rainfall .....	39
5.3 Discussions .....	43
CHAPTER 6 CONCLUSIONS .....	45
REFERENCES .....	46

## **List of Tables**

Table 2.1 Showing the value of F.O.S for various types of reinforcement .....	12
Table 3.1 Properties of geosynthetics used in the study .....	16
Table 5.1: Uniformity Coefficient and Curvature Coefficient of soil sample .....	26
Table 5.2 Specific Gravity of soil .....	27
Table 5.3 Atterberg Limits.....	27
Table 5.4 Water Content and Dry Density relation for compaction test .....	28
Table 5.5 Results of Compaction test .....	29
Table 5.6 Values of cohesion (c) and internal friction angle ( $\phi$ ).....	29
Table 5.7 Showing values of different soil properties .....	30



## List of Figures

Figure 1.1 Slope failures due to rainfall.....	2
Figure 1.2 Mechanism of precipitation-induced slope instability .....	3
Figure 1.3 Showing different combination to form geocomposite and their functions .....	6
Figure 3.1 Location of study area .....	14
Figure 3.2 Geometry of the study slope having a slope inclination of 29.36°.....	15
Figure 3.3 Geometry of the study slope having a slope inclination of 37.65°.....	15
Figure 3.4 Geometry of the study slope having a slope inclination of 42°.....	16
Figure 3.5 Variation of Monthly Precipitation .....	17
Figure 4.1 Schematic representation of the stages involved in the study .....	18
Figure 4.2 Set of sieves arranged and placed in a mechanical shaker .....	19
Figure 4.3 Shows the Direct Shear Test Assembly.....	22
Figure 4.4 HCF and SWCC for study location .....	24
Figure 4.5 Input parameters for reinforcement loads.....	25
Figure 5.1 Particle size distribution curve .....	26
Figure 5.2 Variation of water content with No. of blows .....	28
Figure 5.3 Variation of Dry density with water content .....	28
Figure 5.4 Mohr- Coulomb Failure envelope .....	29
Figure 5.5 For slope with slope angle 29.36° F.O.S is more than 1 before rainfall .....	31
Figure 5.6 For slope with slope angle 37.65° F.O.S is more than 1 before rainfall .....	31
Figure 5.7 For slope with slope angle 42° F.O.S is more than 1 before rainfall .....	32
Figure 5.8 Shear Mobilized vs Shear Resistance for slope angle 37.65° before rainfall.....	32
Figure 5.9 For slope angle 29.36° F.O.S is 1.207 at max. rainfall .....	33
Figure 5.10 For slope angle 29.36° F.O.S is 1.362 at min. rainfall .....	34
Figure 5.11 For slope angle 29.36° F.O.S is 1.178 at avg. rainfall.....	34
Figure 5.12 For slope angle 37.65° F.O.S is 0.992 at max. rainfall .....	35
Figure 5.13 For slope angle 37.65° F.O.S is 1.085 at min. rainfall .....	35
Figure 5.14 For slope angle 37.65° F.O.S is 1.137 at avg. rainfall.....	36
Figure 5.15 For slope angle 42° F.O.S is 0.928 at max. rainfall .....	36
Figure 5.16 For slope angle 42° F.O.S is 1.011 at min. rainfall .....	37
Figure 5.17 For slope angle 42° F.O.S is 1.015 at avg. rainfall.....	37
Figure 5.18 Shear Mobilized vs Shear Resistance for slope angle 37.65° after rainfall.....	38
Figure 5.19 Comparison between slope angle and factor of safety at different rainfall intensities	

.....	38
Figure 5.20 For slope angle $37.65^\circ$ F.O.S is 1.210 with 3 layers of geosynthetic.....	39
Figure 5.21 For slope angle $37.65^\circ$ F.O.S is 1.243 with 4 layers of geosynthetic.....	40
Figure 5.22 For slope angle $37.65^\circ$ F.O.S is 1.278 with 5 layers of geosynthetic.....	40
Figure 5.23 For slope angle $37.65^\circ$ F.O.S is 1.315 with 6 layers of geosynthetic.....	41
Figure 5.24 For slope angle $42^\circ$ F.O.S is 1.102 with 3 layers of geosynthetic.....	41
Figure 5.25 For slope angle $42^\circ$ F.O.S is 1.122 with 4 layers of geosynthetic.....	42
Figure 5.26 For slope angle $42^\circ$ F.O.S is 1.151 with 5 layers of geosynthetic.....	42
Figure 5.27 For slope angle $42^\circ$ F.O.S is 1.179 with 6 layers of geosynthetic.....	43

# CHAPTER 1 INTRODUCTION

## 1.1 General

Whether man-made or natural, a slope refers to an inclined ground surface. Stability of a slope is the capacity of an inclined surface to sustain the external forces and its own weight without failing. The fundamental concepts of rock/soil structure, and geotechnical engineering, are applied to the stability of slopes. Case studies involving the behaviour of the slope have contributed in a great understanding of the stability of slopes evaluations, the establishment of complex constitutive mathematical equations/models, an understanding of lab work as well as in-situ assessment limitations, in addition to the construction of new equipment to evaluate the slope's response.

When the stability requirements fail to be fulfilled, the rock or soil mass of the slope can undergo a downward shift that could be catastrophically quick. The term for this type of event is failure of slope or landslide. A landslip can be initiated due to an earthquake, precipitation that exceeds the pressure caused by pore water, or the deterioration of the surface mechanical properties. Every year, failure of slopes systemically deteriorates human constructions and can cause numerous deaths.

In several regions of the world, slope instability has become a pervasive problem that annually results in innumerable deaths. Even though slope failure can occur as a consequence of development operations, numerous instances of slope failure have been observed on both non-excavated soil slopes and explored slopes due to the penetration of rainwater into the stable slopes. This is due to a reduction in suction matrix values or an increase in pressure induced by pore water as water percolates into unsaturated soil in a slope. Utilising geosynthetics on slopes is an excellent method for achieving slope stability. Alternately, it is possible to combine the drainage properties of a geotextile that is non-woven with the stiffness or strength of a more robust reinforced geosynthetic, such as geogrid, to produce a mixed geosynthetic, also known as a geocomposite.

The province of Shimla is often impacted by landslides, which are regarded among one of the nature's most destructive hazards. When it overflows in the region during monsoon seasons, the scenario becomes so dire. Large quantities of surface materials moving downslope under the impact of gravity pose a significant environmental concern in the study area. Slow motion can be expensive, but it poses a lower risk of mortality than rapid motion, which causes damage

and death. On rain-soaked, poorly drained slopes, investigation of an appropriate approach for minimising the pressure of pore water and soil deformation was done. A hybrid geosynthetic has been produced by combining the permeability of the non-woven geotextile along with the strength of the woven geogrid (Bhattacharjee and Viswanadham, 2019). The highland ecosystem constitutes one of the worst-affected ecosystems in the world, as it is vulnerable to a variety of natural and anthropogenic hazards and environmental issues (Martha et al., 2012). Landslides are among the most destructive events that occur in mountainous regions and alter the geomorphology of the surface (Gupta and Joshi, 1990). Figure 1.1 depicts the failures of slopes that occur due to rainfall.

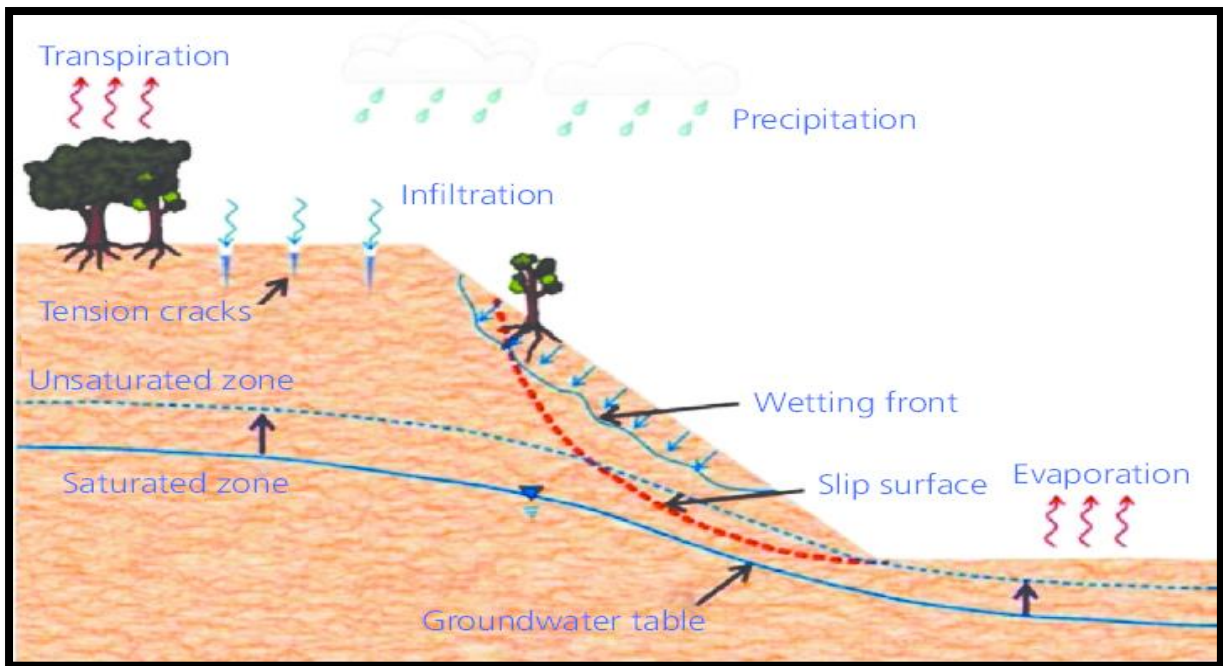


Figure 1.1 Slope failures due to rainfall (after Rahardjo et al., 2007)

## 1.2 Causes of Failure of slope

The failure of the slopes can occur due to the natural or human-induced factors, or both. Gravitational forces which tend to destabilise the ground, saturation of water, erosion, seismic activity (e.g., earthquakes), the abrupt increase in the groundwater level, and weathering caused by the cycles of freezing and thawing are all natural causes of landslides.

A high concentration of water serves as one of the greatest causes of landslides. Heavy precipitation, snowmelt, or variations in the ground water level, all of this can result in the saturation of water. Shear strength of the soil is diminished by soil saturation. In particular, it reduces the normal effective stress acting along the granules, thereby decreasing the frictional resistance. Mohr-Coulomb failure criterion states that the shear strength of the soil corresponds to the normal effective stress as follows:

$$S = C + \sigma_n \tan \phi \quad (1)$$

$$\sigma_n = \sigma - u \quad (2)$$

Here, S corresponds to shear strength,  $\sigma_n$  is normal effective stress, u is the pressure caused by pore water,  $\sigma$  gives total stress, C is cohesion, &  $\phi$  is angle of friction.

### 1.3 Effect of rainfall on the stability of slope

During rainfall, numerous slope collapses occur on steeply soil slopes having a high groundwater level. Steep residual soil slopes are typically characterised by a considerable depth of an unaltered soil layer above the water level. The negative pressure created by the water in the pores in unsaturated soil is significantly affected by the boundary flux modifications (i.e., permeability, evaporation, and transpiration) caused by climatic conditions that varies. Alternatively, negative pore-water pressure adds to that of the unsaturated soil's shear strength. As water percolates into a slope, pore-water pressure increases (matric suction decreases), while the enhanced shear strength produced by matric suction diminishes or disappears, making the slope more prone to the failure. Both transpiration and evaporation will restore the slope's lost matric suction. In another word, unsaturated region is a connection between the slope and the atmosphere, and consequently, the safety factor of the slope is dynamically influenced by the climate change. Figure 1.2 depicts the process of the precipitation-induced slope failure with the effect of infiltration, evaporation & transpiration.

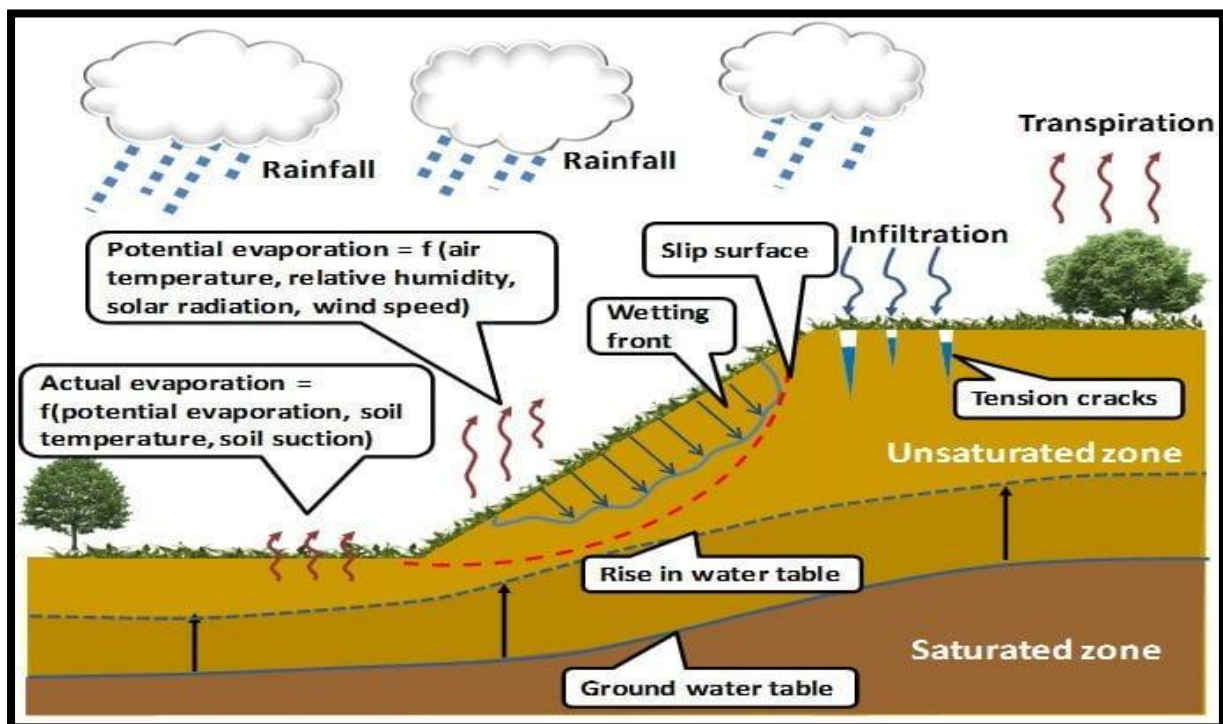


Figure 1.2 Mechanism of precipitation-induced slope instability (after Rahardjo et al., 2012)

## **1.4 Overview of Slope/W of GeoStudio software**

SLOPE/W employs the limit equilibrium method to evaluate the stability of a given geometry. In limit equilibrium technique, a trial slip interface slices a sliding mass into several vertical segments. An iterative method is used to calculate (prior to failure) the variable that determines the shear strength of each segment should be reduced in order to make the sliding mass nearly on the state of static equilibrium. This reduction factor is referred to as the safety factor. Moment as well as force equilibrium could be employed to determine equilibrium. Consequently, SLOPE/W computes two safety variables: one for moment equilibrium while another one for horizontal force stability. In the current investigation, the interslice force operation is represented as half of the sine function using the Morgenstern-Price method.

## **1.5 Different methods of analysis**

### **1.5.1 Limit Equilibrium Method**

The limit equilibrium evaluation is one of the typical methods for determining the level of stability of slopes. According to the concept of equilibrium, a stable slope signifies a state in which all the forces operating on the slope remain in equilibrium. The analysis entails sectioning the slope and evaluating the stability throughout each section separately.

In limit equilibrium evaluation, the safety factor (FS) should be utilised to determine the slope stability. Factor of safety represents the proportion of the slope's resisting forces by its driving forces. When the safety factor exceeds more than one, the slope is deemed stable; otherwise, it is deemed unstable.

Limit equilibrium evaluation is one of the popular methods for evaluating the stability of slopes, though it has limitations. It presumes the soil attributes are homogeneous as well as isotropic, which might not always be the case. It also disregards the results of the pressure of pore water, which could have a significant effect on slope stability. As a result, other analysis techniques, like FEA (finite element analysis) as well as finite difference method (FDM), can be utilised to supplement the outcomes derived from limit equilibrium analysis.

### **1.5.2 Morgenstern Price method**

The Morgenstern-Price approach is an analysis technique for stability of slope that considers the pressure of pore water produced by the penetration of water into the slope. In the 1960s, Canadian geotechnical engineers Zdenk Morgenstern and William Allen Price developed this method.

The method assumes that a slope could be subdivided into a number of slices, each of the slice possessing a distinct factor of safety over failure. After deducting the pressure created by pore

water from the total stress, the method requires determining the effective stresses for each slice, which represent the stresses appearing on the soil particles. The degree of safety against the failure is then calculated for each slice through the proportion of the shear strength within the soil with the shear stress exerted on the slice.

The Morgenstern-Price method is applicable for analysing slopes of any kind, including those with complex geometries along with soil profiles. It has been implemented in numerous slope stability evaluation software applications and is commonly utilised in practise. In practise, however, it is not always the case that the slope's soil properties as well as pressure caused by pore water remain uniform throughout the whole slope.

### **1.5.3 Finite Element Method**

FEA is a mathematical method for analysing and predicting the behaviour of complex systems of engineering. It entails decomposing a system into smaller, less complex components called finite elements and then modelling the behaviour of each element using mathematical equations as well as numerical methods. The equations are simultaneously solved for each element in order to derive an outcome for the whole system.

In geotechnical engineering, the finite element analysis is frequently employed to model the behaviour of soil and rock formations, particularly under conditions of complex geology. FEA can be used to analyse, among other things, slope stability, foundation behaviour, tunnelling, and excavation issues.

FEA necessitates a thorough comprehension of the the study of geometry, boundary constraints, material characteristics, and loading circumstances of the being examined system. The precision of the results is contingent on the precision of the input factors along with the model's complexity. FEA is an effective tool, but it requires substantial computational resources, specialised software, and knowledge of numerical methods as well as computer programming.

### **1.6 Geosynthetics**

Geosynthetics are the essential components of a structure or system that is used to accomplish various engineering goals or objectives. Typically, Geosynthetics products are composed of polymeric materials. Geo refers to the planet Earth, which represents the soil, while synthetics refers to polymeric or synthetic materials. Geosynthetics, as implied by its name, refers to the synthetic materials used to enhance the soil's stability.

There are numerous applications for geosynthetics materials, including reinforcement, the filtration process, separation, drainage, and water barrier.

Geosynthetic materials are utilised in construction initiatives involving soil/rock. In the domain of civil engineering, projects involving soil such as roads, railways, dams, hydraulics, retaining walls, canals, marine structures, foundations, and embankments utilised this material extensively.

Due to its synthetic nature and high durability, geosynthetics is the most appropriate material for underground applications. The main objective of geosynthetics is to enhance the stability and strength of soil while lowering construction costs. When two or more geosynthetics are used it is referred as Geocomposite or hybrid geosynthetic. Figure 1.3 depicts the functions and different combinations of geocomposite.



Figure 1.3 Showing different combination to form geocomposite and their functions  
([www.civilengineeringweb.com](http://www.civilengineeringweb.com))

### 1.7 Objectives of current study

The present study's objectives are as follows:

1. To analyse the impact of variation of angle on the slope stability.
2. To analyse the effect of rainfall on the stability of slopes using numerical modelling.
3. To study the effect of geosynthetics for the stability of slopes.



## CHAPTER 2 LITERATURE REVIEW

- **Gupta and Joshi, (1990)** in their study used a GIS (Geographic Information System) methodology, and explored the creation of a technique for assessing the risk of landslip hazards. The technique was implemented to Ramganga basin in Lower Himalayan Mountains, and the research is founded on multiple data sets. Several parameters, including lithology, geography, distance from a major tectonic-shear zone, and orientation, are related to landscape activity. Using data from 522 landslips in four designated sub-basins, the "landslide nominal risk factor" (LNRF) was established and calculated for every significant parameter. The terrain has been allocated varying weights based on the LNRF and incorporated into an ordinal scale in order to identify regions with low, moderate, and high landslip hazard.
- **Rahardjo et al., (2001)** stated that both daily rainfall and preceding rainfall are significant precipitation triggers for the appearance of landslides. As prior precipitation enhances the soil's permeability as well as subsequent storm events can initiate a landslip, the daily or maximum precipitation by itself cannot be utilised as a landslip effect. A 5-day antecedent precipitation greater than 60 mm plus a daily precipitation higher than 90 mm (i.e., cumulative rainfall greater than 150 mm over a period of six days) seems sufficient to have caused land collapses.
- **Rahardjo et al., (2007)** stated that the rainfall-induced failure of slopes is a prevalent geotechnical issue in tropical regions with abundant residual soils. Despite the fact that the value of infiltration of rainwater in triggering landslips is widely acknowledged, various conclusions had been reached regarding the respective roles of preceding rainfall in triggering landslides. Through a series of parametric experiments, the significance of properties of soil, intensity of rainfall, initial water table, and geometry of slope in causing instability of uniform soil slope under varying rainfall was determined. Soil characteristics and intensity of rainfall were discovered to be the primary variables governing the instability of slopes that result from rainfall, while the initial water level position as well as geometry of slope played only a minor role. The outcomes of the research also stated that, for a particular duration of rainfall, there existed a threshold intensity of rainfall that would generate a minimum safety factor.
- **Sharma and Kumar, (2008)** carried out a GIS-based landslip hazard zonation for a region in the Himalayas that is tectonically active and under the pressure for accelerated economic growth. Using topographic maps, images from satellites, published geological maps, and

ground truth, thermal layers of the slope, fault, geology, use of land, drainage, and embankments were created. 54% of the observed landslides occurred in zones with Very high as well as High landslip calamity, where 24% of the entire area is located. According to the research, the two most significant factors are vicinity to faults along with drainage. Observations made in the field indicate that the breakdown of rocks and the existence of extraterrestrial as well as tectonic shear were the main factors that cause the occurrence of instability, while breakdown being especially prevalent along the joints and zones of water flow. Precipitation is a significant causative factor.

- **Tan et al., (2011)** described that the infiltration of precipitation is a significant factor influencing stability of slope. To examine the impact of precipitation concerning the viability of a highway slope, a typical sliced slope of a highway in a monsoon region was chosen for the research. On the basis of saturated - unsaturated drainage principles and solid-liquid research, the characteristics of seepage, pressure caused by pore-water, stress along with settlement of a highway slope under two distinct intensities of rainfall as well as duration situations are analysed. Simultaneously, modified Mohr-Coulomb parameters and the 2-D limit equilibrium technique were utilised to evaluate the slope's factor of safety. With increasing rainfall duration and intensity, the extent of the unsaturated zone reduced, whereas the saturated region expanded, the pressure caused by pore-water, settlements, and negative shear stresses on the outermost layer of the slope increased. The slope's safety factors also decreased as rainfall duration and intensity increased and were all less than 1.0. The slope was mitigated by applying reinforcement of an anchor-shotcrete with an adhesive suspended net bolt. Monitoring on the ground revealed that this reinforced slope was stable after prolonged heavy rainfall. Thus, reinforcement of an anchor-shotcrete is an effective technique for reinforcing slopes in wet areas.
- **Zhai and Rahardjo, (2012)** described that the soil–water characteristics curve (SWCC) comprises the fundamental data necessary to describe the mechanical behaviour of unsaturated soil. Certain parameters, including the air-entry value, slope at the location of inflection, remaining water content, & residual suction, were typically employed to characterize the SWCC and some other related properties, like its shear strength as well as permeability. At this time, these parameters are selected using the subjective and time-consuming graphical method. This paper proposes equations for calculating these parameters and discusses the relationship among SWCC factors as well as fitting factors. These equations may be implemented in computational analyses in lieu of the conventional graphic approach to produce consistent outcomes.

- **Rahardjo et al., (2012)** described that the mechanism of rainfall-induced failures of slopes requires an understanding of the mechanics of unsaturated soils. Utilising the fundamentals of unsaturated soil structure, the changes in the pore-water pressure and safety factor of a slope during precipitation could be accurately evaluated. Rainfall is integrated into seepage analyses by applying a flux boundary to the slope's surface. For seepage analyses, the SWCC (soil-water characteristic curve) along with permeability functions were among the most important parameters. Utilizing unsaturated soil mechanics, the capillary barrier system minimizes seepage into slopes and prevents failure of slopes. If a slope fails due to precipitation and the groundwater level is extreme, the implementation of horizontal drains can be used to repair the slope.
- **Li et al., (2013)** used centrifuge experiments and 2-dimensional finite element methods, to check the stability of elevated and steep geosynthetic strengthened slopes under their own weight is studied. Two centrifuge model experiments were carried out to investigate the mode of failure or trend by analysing the differences in settlement along with lateral displacement, upward stress, and horizontal stress of representative models. On the basis of the basic variables of the centrifuge layout evaluations, 2-D FEM (finite element models) were developed to compare with that of centrifuge model outcomes. A comparison of calculated centrifugal simulation test outcomes established the validity of the finite element method-based established model. In addition, the remainder of their study focused on numerical evaluations of performance and systems of the geosynthetic reinforced slopes, specifically the effect of the strength along with the stiffness of the geosynthetic over the slope's subsidence, lateral displacement, and both vertical and lateral stresses. Results indicate that geosynthetic reinforcements had a significant impact on enhancing stability of slope, and study findings delivers the theoretical foundation for creating a steep geosynthetic reinforced slope.
- **Collins et al., (2014)** investigated the incorporation of geofibers as well as nontraditional additives for sandy silt. Several combinations consisting of geofibers and unconventional additives were evaluated using a combination of field along with laboratory investigations. The initial field tests yielded somewhat inconclusive results, so a three-part plan was developed to learn further about embankment stabilization using geofibers as well as nontraditional additives. This plan included evaluating the critical shear stresses for the processed soils, assessing the influence of additives on the plant structure of grass grown at the field location, and building a laboratory-scale gradient to measure loss following a significant erosion incident.

- **Kahlon et al., (2014)** described that in Himachal Pradesh, the appearance of landslides is prevalent and widespread. In addition to an increase in the annual and decadal instances of landslides, there is rise in the frequency of years with an extremely high occurrence over each decade. The frequency of landslides in Shimla, Solan, Kinnaur, & Mandi districts during the past forty years has been exceptionally high. Rainfall with high intensity, particularly during monsoons, serves as one of the primary causes of such occurrences. The natural conditions of the state, such as unstable precipitous slopes, weak geological structure, and heavy precipitation, were the primary causes of failure of slopes. Increased susceptibility of these geologically young and unstable precipitous slopes has raised, however, as a result of human activity such as the building of roads, the expansion of towns and related developmental endeavours, deforestation, and alterations in agricultural patterns. This is especially true in the landslide-prone districts of Chamba, Shimla, Kullu, and Lahaul & Spiti Valley, where massive road construction and enlargement activities are currently underway to help projects of hydro-power as well as transportation facilities.
- **Krishnan and Vasantha, (2015)** on the basis of the USLE, an effective fuzzy logic-based system that requires fewer input variables was devised for tracking erosion risk in areas with constant precipitation. This model proved to be in fair agreement with actual measurements in the field when compared to them. Additionally, it was noted that the framework is consistent with previous outcomes in similar designs. The F-SEM & F-CGM models are created for diverse types of soil. Projections were generated for both fixed and variable intensities of precipitation. The F-CGM is devised for forecasting of CG for a specific combination of precipitation, soil type, as well as slope gradient in order to achieve an acceptable minimal soil loss. The opening dimensions of both woven as well as nonwoven types were evaluated as the primary criterion for determining the optimal CG.
- **Viswanadham and Bhattacharjee, (2016)** stated that every year, rainwater infiltration-related slope instability costs huge amount of money in infrastructure damage and many lives worldwide. The issue gets worse if the soil on the entire slope has low permeability and is unable to relieve the pressure that rainfall-generated pore water causes. In recent years, the lack of high-quality backfill material has necessitated the use of accessible, low-permeability soil in the development of reinforced slopes and walls. A feasible choice is the incorporation of geocomposites into the slope to provide drainage as well as the reinforcement actions required to maintain the slope's stability in the face of precipitation. In their study used Geostudio software, the impact of precipitation on seepage properties and worldwide slope stability with and without geocomposites was investigated

numerically. The placement of geocomposite layers at the base of the slope proved to be the most effective when compared to the intermediate and top positions. Utilising dual-function geocomposites on slopes exposed to precipitation eliminates the need for costly high-permeability fill materials, saving money on the project.

- **Merat et al., (2017)** in their research seeks to examine the impact of climate on stability of slope. The climate has been expressed by precipitation rate and time frame, and the long-term stability of a dry slope in the natural landscape was assessed using the key indicator "safety factor." The slope's stability was analysed using the 2015 version of the PLAXIS2D finite elements software. The safety factors were evaluated using completely coupled flow-deformation assessments and examined to the various controlling parameters: intensity of rainfall, duration of rainfall, slope angles, characteristics of soil, as well as soil's hydraulic conductivity. In this paper, the outcomes were addressed and used to validate the relationship between landslide and climate impacts considered in this study.
- **Singh and Srivastava, (2017)** investigated the response of unreinforced and soil-nailed slopes to varying static surcharge loads. The slopes were built with sand-sized soil at an assumed soil slope inclination of 60 degrees with the horizontal plane. To observe the load versus settlement behaviour, a variety of inert loads were applied to a bearing plate placed on the slope's crest. Then, these soil slopes were reinforced by placing aluminium hollow tubes that serve as soil anchors at three distinct inclinations of 0°, 15°, and 30°, with the horizontal plane maintaining a vertical and horizontal spacing of 0.1m. In this research, the impact of soil nail patterns within the soil gradient is also examined. There were square, diamond, and staggered nail arrangements. Using strain gauges, in their study they also determined the stress and strain generated in the various positions of the installed nails during the following phases of loading. Observations indicate that nails placed at 0° were more efficient than nails placed at 15° and 30° in stabilising slopes. In addition, fasteners installed in a staggered pattern proved to be the most effective.
- **Mudgal et al., (2018)** stated that it is evident from the triaxial assessments that the geotextile increases the integrity of the Yamuna sand. The adhesion of non-woven geotextile to Yamuna sand was greater than that of woven geotextile, however, the strength of Yamuna soil was enhanced more when it is reinforced using woven geotextile. Therefore, it can be stated that the appropriate geotextile can be utilised contingent on the use of geotextile. Consequently, significant increase in the shear strength, woven geotextile needs to be utilised for reinforcement.

- **Bhattacharjee and Viswanadham, (2019)** investigated an appropriate technique to minimise pore-water pressures as well as deformations in weakly draining, rainfall-exposed soil slopes. As a hybrid geosynthetic material, the strengthening purpose of the woven geogrid combined with discharge characteristic of the non-woven geotextile. On silty-sand slopes, a combination of centrifuge experiments was performed using an in-flight precipitation simulator. Due to the lack of seepage or reinforcing features, the unreinforced slope experienced toe failure and infiltration of rainfall. Due to insufficient drainage, geogrid-reinforced slopes felt significant displacements and rising phreatic levels with the precipitation, as well as 38%–48% geogrid straining. Even though the rise in phreatic levels reduced significantly on geotextile-reinforced slope, rainfall eventually caused failure of slope due to insufficient reinforcement. Further, a seepage evaluation was done to determine the impact of geogrids, geotextiles, & even hybrid geosynthetics on modulating the slope safety factor with precipitation.
- **Sharma et al., (2019)** investigated that to increase the effectiveness of the reinforced subsoil should have reinforcement set at regular intervals. The pull-out resistance of geotextiles is created through an interface mechanism of friction. Both interface friction & resistance of the soil against lateral elements can contribute to the development of geogrid pull-out resistance. In the steady case, the slope is stabilised by 7 successive layers of the geotextile reinforcement, with the centre-most layer extending twice as far as other layers, & three layers of geogrid strengthening. For slope stability in the dynamic situation, 1 additional layer of geotextile as well as 2 extra layers of geogrids must be provided. F.O.S with reinforcement is shown in table 2.1.

Table 2.1 Showing the value of F.O.S for various types of reinforcement

Reinforcement	Morgen price/ Spencers method
Without reinforcement	1.015
Geotextiles in 3 layers	1.113
Geotextiles in 7 layers	1.235
Extended geotextile	1.379
Geogrid	1.336

- **Ering and Babu, (2020)** described a procedure for identifying critical rainfall on slopes impacted by precipitation. In places where landslip occurrence is substantial and landslip forecast alone is unacceptable, clarification of current landslides triggered by precipitation

needs incorporation of possible factors that trigger due to precipitation. This can be achieved by identifying slope-critical precipitation. Although numerous precipitation thresholds in their research provide a range of critical precipitation values for a gradient, it was hard to determine from these thresholds the precise class of precipitation that operates as the critical precipitation. In their research, a rainfall threshold was constructed utilising the prediction of landslides caused by rainfall (FLaIR) method, historical landslide data, and precipitation infiltration evaluations.

- **Tiwari et al., (2021)** described that due to the swelling nature of expansive soils, the upward pressure on structures built on them is greater. Numerous conventional treatment techniques created to counteract the swelling and shrinking properties of expansive soil were considered inefficient and time-consuming for use in embankment. Geotextiles (GTs) were adopted for filtration as well as separating medium, but their impact on the swelling pressure & shear properties of expansive subgrade soil was not thoroughly investigated. The purpose of their study was to solve these problems with employing GT in regulating swelling behaviour, remove moisture, and offer support to the surface of soil. Constant volume swelling pressure along with direct shear as well as unconfined compressive strength experiments were utilised, respectively, to determine the swelling pressure and shear strength. Studied were the effects associated with one-layer, two-layer, as well as three-layer GTs at differing heights. The GT layer's greater tensile strength reduced the surge pressure by avoiding the internal movement of soil and causing in-plane drainage. Consequently, it was observed that soil-geotextile interfacial interactions contributed to the enhancement of shear strength.
- **Ferreira et al., (2022)** employed a creep rupture testing protocol to investigate the long-term tensile behaviour of a high-strength geotextile typically employed for soil reinforcement. In order to analyse the chemical potential as well as degradation of environment caused by reclaimed C&D materials on this geosynthetic material's long-term effect, results of tests on fresh and exhumed specimens were analysed. Utilisation of intact samples for creep tests can therefore be regarded as a secure method for predicting long-term integrity of geotextile. Exposure of the geotextile to either reclaimed construction and demolition debris or natural soil caused same effects upon its creep strain as well as rupture behaviour.

## CHAPTER 3 STUDY LOCATION

### 3.1 Area of Study

The research location is close to the Bagawat village link route in India's Himachal Pradesh district of Shimla. Figure 3.1 illustrates the position of the survey area using Google Earth. Shimla Tehsil is located between 30°593 & 31°1410 North latitude and 76°5819 & 77°1921 East longitude. The entire area of Shimla Tehsil is 36,830 hectares (Prakasham et al., 2019)



Figure 3.1 Location of study area

### 3.2 Description of the Field of Study and properties of materials

For the slope stability analysis, three slopes were considered: a gentle slope, an actual slope, and a critical slope, with slope angles of  $29.36^\circ$ ,  $37.65^\circ$ , and  $42^\circ$ , as depicted in Figures 3.2, 3.3 and 3.4. For the stability analysis, an 80-82 m tall failure slope is being considered. The actual angle of the slope was  $37.65^\circ$ , and two other slope angles, one lower to that of the actual slope angle ( $29.36^\circ$ ) and the other higher to that of the actual slope angle ( $42^\circ$ ), were considered to evaluate the effect of rainfall on such slopes and their stability following rainfall. Properties of hybrid geosynthetic are depicted in Table 3.1.



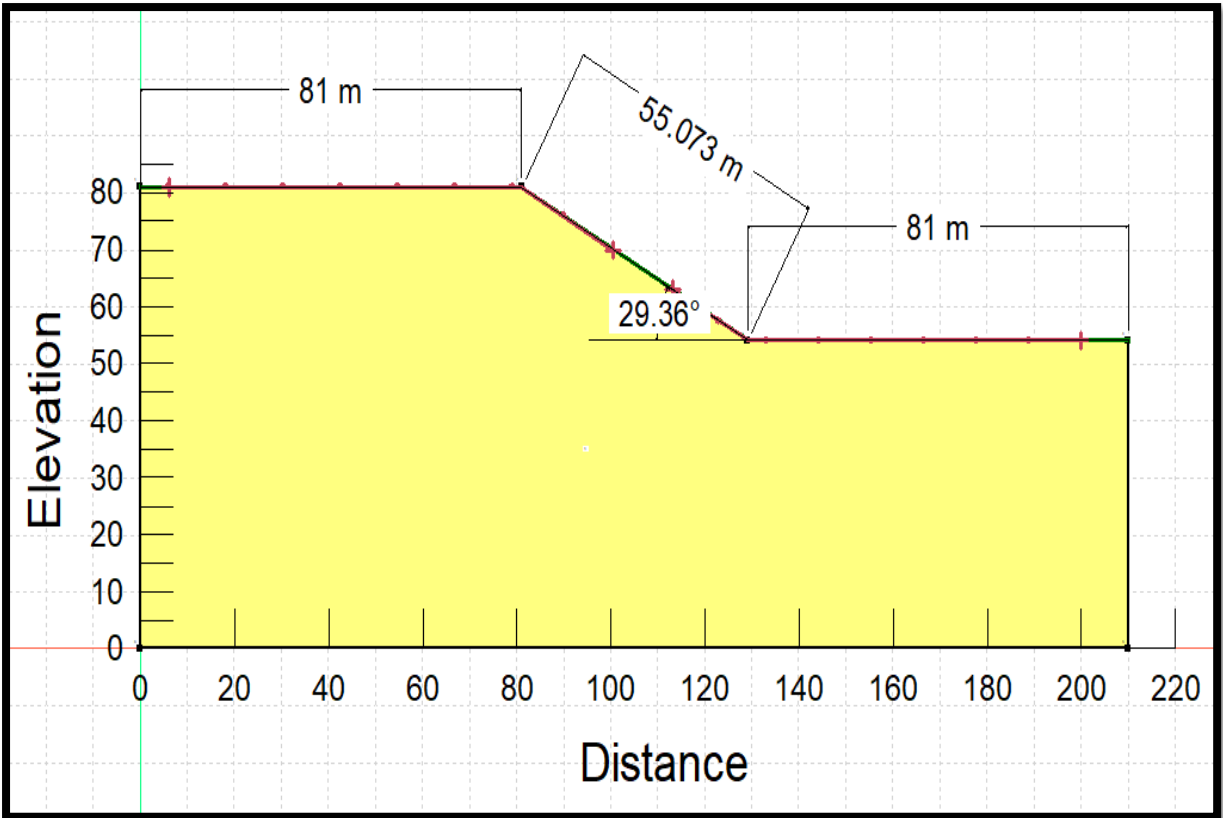


Figure 3.2 Geometry of the study slope having a slope inclination of 29.36°

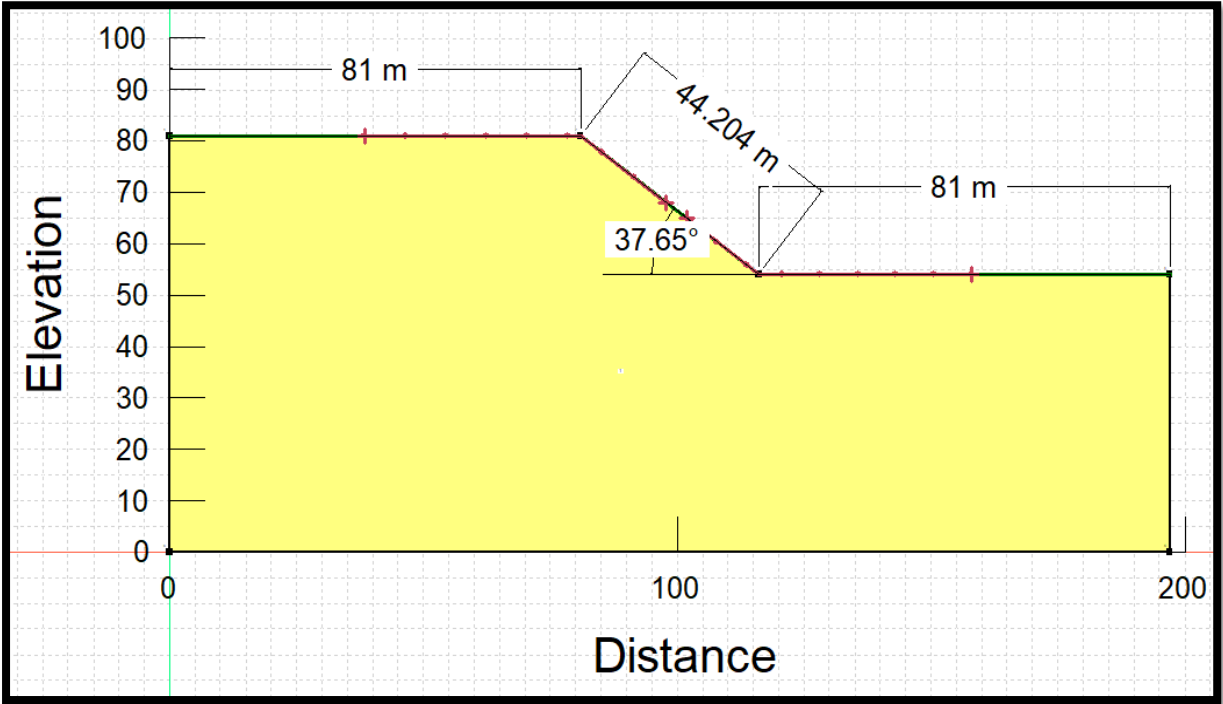


Figure 3.3 Geometry of the study slope having a slope inclination of 37.65°

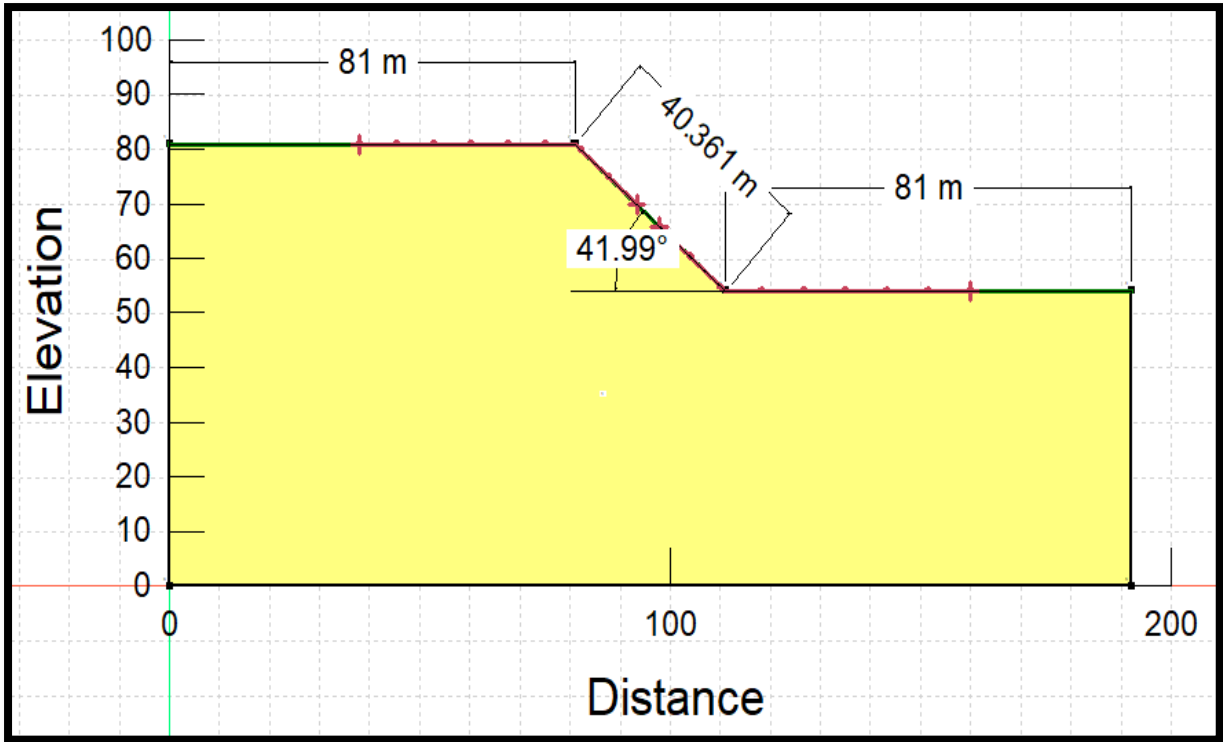


Figure 3.4 Geometry of the study slope having a slope inclination of 42°

Table 3.1 Properties of geosynthetics used in the study (Vishwanadham and Bhatacherjee, 2016)

S.No.	Geosynthetic Property	Values
1.	Tensile Load (kN/m)	55.35
2.	Bond skin friction (kPa)	12.5
3.	Normal permeability coefficient (m/sec)	$12.59 \times 10^{-5}$
4.	Tangential permeability coefficient (m/sec)	$7.975 \times 10^{-4}$

### 3.3 Rainfall Characteristics

The principal factor contributing to landslides occurring in the Shimla region is rainfall. The monsoons influence the climate of the region, with the heaviest rainfall occurring between the months of June and September. Due to its location amid the Lesser Himalaya, the research region encounters orographic precipitation. Consequently, precipitation & slope orientation are critical variables pertaining to the emergence of the landslides. The regional centre of the Indian Meteorological Department in Shimla provided data for monthly precipitation variation as shown in Figure 3.5

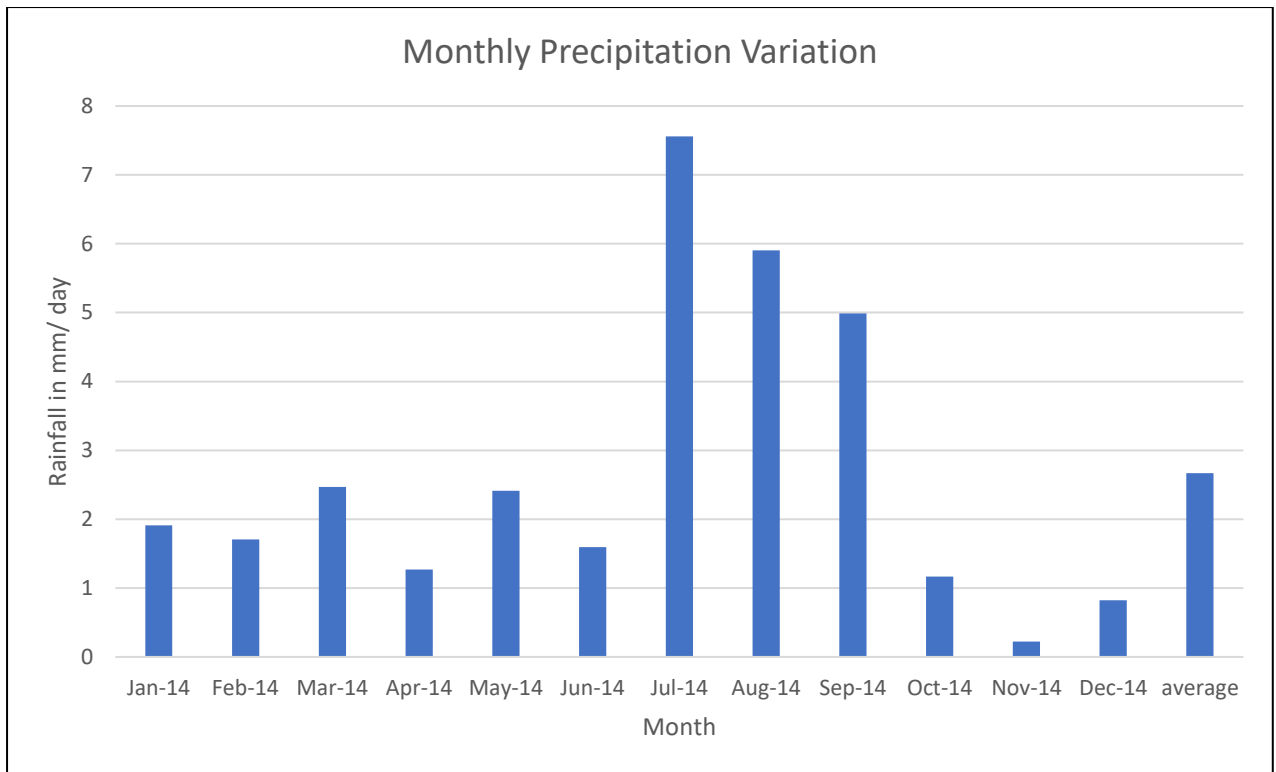


Figure 3.5 Variation of Monthly Precipitation (Source: IMD)

## CHAPTER 4 METHODOLOGY

In this chapter the various methods used for the study are explained and with the help of the flowchart the sequence of the methodology followed is shown below:

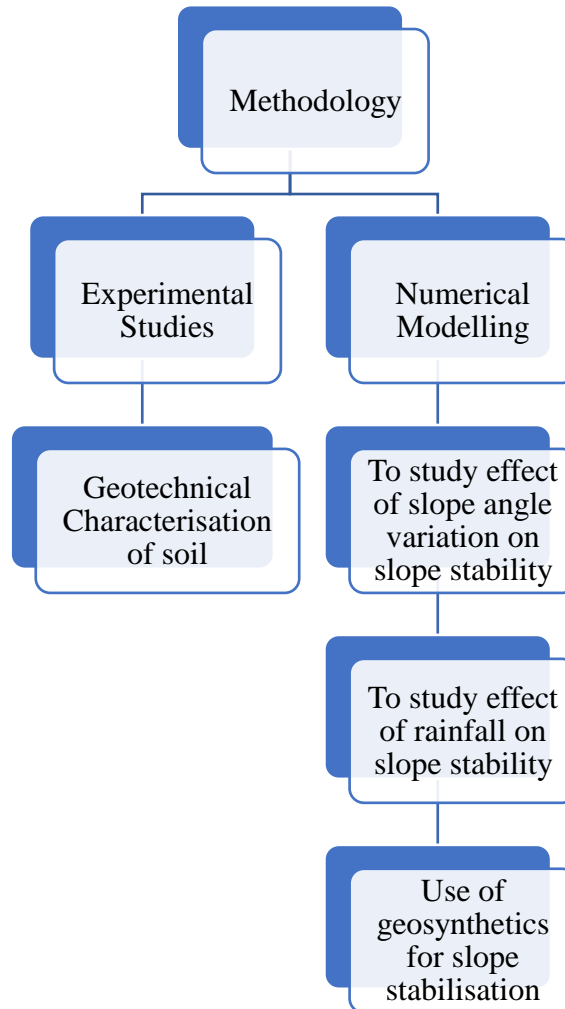


Figure 4.1 Schematic representation of the stages involved in the study

### 4.1 Experimental Studies

Various laboratory investigations were done on soil to know the characteristics of the soil and different methodologies for different tests are discussed below:

#### 4.1.1 Particle Size Distribution Analysis

The particle size evaluation test was carried out to figure out the proportion of every grain size evident in a sample of soil as per IS:2720 (Part 4)-1985, and the outcomes of the test are used to create the distribution curve of grain size. These data were used to categorise and foresee the behaviour of soil. The two common methods for evaluating particle size distribution are:

- Sieve method for grain size greater than 0.075 millimeters.
- Hydrometer method for grain size less than 0.075 millimeters.

Sieve testing is a technique used to identify the distribution of the size of grains of soil in relation to particle sizes larger than 0.075 mm. This is typically used for gravel and sand, but it cannot be used by itself to determine the percentage of particle sizes of finer soil. This test employs sieves formed by wires that are woven with shape of square. A known quantity of material, whose quantity is based on the largest size of material, is positioned at the top of a series of stacked sieves (topmost sieve possesses the biggest openings, and the opening dimensions reduce with each subsequent sieve down towards bottom sieve that has least size screen) and shaken for some time. Following the shaking of the material across the stacked sieves, the total material retained on every sieve is measured.

For particle size analysis, 1 kg of soil sample was taken and passed through a set of sieves i.e., 4.75 mm, 2 mm, 1.18 mm, 600  $\mu$ , 425  $\mu$ , 300  $\mu$ , 150  $\mu$  and 75  $\mu$  sieves with the help of mechanical sieve shaker. Then after shaking for some time, then weight of the soil sample retained on every sieve is taken and with the help of this gradation analysis chart is being made. The data could also be used to establish relationships between porosity and packaging. The soil is classified based on the information derived from the analysis of particle sizes (uniformity indicator  $C_u$ , the coefficient of curvature  $C_c$ , effective size  $D_{10}$ , etc.)



Figure 4.2 Set of sieves arranged and placed in a mechanical shaker

#### 4.1.2 Determination of Specific Gravity

Specific gravity represents a dimensionless quantity described as the ratio of soil solids density to water density at a given temperature. Using the pycnometer method, specific gravity of a soil sample was evaluated in accordance to IS: 2720 (Part 3/Sec 2) -1980. A 100-gram oven-dried specimen is analysed in this test. Calculate and record the pycnometer's unfilled weight, M<sub>1</sub>. Fill that pycnometer with 100 grammes of oven-dried specimen and weigh it as M<sub>2</sub>. Fill the pycnometer with distilled water up to the top, and weigh it as M<sub>3</sub>. Empty, clean, and fill the pycnometer to the mark with water. This must be measured as M<sub>4</sub>. The specific gravity will then be determined using the following relationship:

$$G = \frac{M_2 - M_1}{(M_2 - M_1) - (M_3 - M_4)}$$

#### 4.1.3 Atterberg Limits Test

The Atterberg limits, referred to "consistency limits," are actually a set of laboratory tests required to ascertain water content when a fine-grained soil shifts state. IS:2720 (Part 5)-1985 was being used to identify the soil's liquid limit as well as plastic limit. For the analysis, 120 g oven-dried sample of soil passing a 425 $\mu$  IS sieve is collected. The sample of soil is thoroughly mixed using enough water to create a homogenous substance. A small quantity of prepared sample of soil was moved to the brass container of Casagrande's Apparatus and levelled to a height of 1 centimetre at the deepest point. Using a suitable grooving instrument, an incision is created in the soil sample while the crank is turned at the rate of two revolutions every second. When the groove created in the soil specimen came into contact at an interval of 12 mm, the no. of blows is recorded. A part of the sample of soil is taken from a position perpendicular to that of the groove, specifically from the region of the groove that came into contact due to flowing, in order to evaluate its water capacity. The experiment is repeated four to five times, and a graph between the log of the no. of blows and the water content is created. The soil sample's liquid limit is analysed by water content which corresponds with 25 blows. After determining liquid limit, approximately 8 g of sample of soil is then rolled between the fingertips on the glass plate until a thread having diameter 3 mm is formed. The procedure is then repeated until cracks emerge on the exterior of the soil thread when it is rolled to a diameter of 3 millimetres. A representative sample of soil is taken from the fractured portion of the thread to assess its moisture content. The determined moisture content reflects the plastic limit of the sample of soil.

#### **4.1.4 Compaction Test**

Compaction is a method of soil densification through the elimination of air voids. The dry density of soil sample is used to determine its degree of compaction. The MDD (maximum dry density) occurs at optimal water content. To determine maximum dry density (MDD) & optimum moisture content (OMC), a graph is drawn among the dry density along with the water content. In this research, Light compaction evaluation has been done in accordance to IS:2720 (Part 7)-1980 to find MDD & OMC. In a light compaction evaluation, a 5 kg sample gets compressed in a compaction mold having volume 938 cc after it passes through a 20 mm IS sieve. Some quantity of soil is taken and is mixed with a fixed percentage of water, consider it as an initial moisture content of soil taken. The specimen will then be packed into the compaction frame in three phases, with each receiving 25 number of blows from a 2.6 kg hammer with a 310 mm falling height. The technique is repeated with the soil sample, this time varying the water content to ascertain the dry density relating to various water contents and to calculate the OMC and MDD. Record the initial water content, the MDD (maximum dry density), and the OMC (optimum moisture content). These values ought to be presented in a standard format.

#### **4.1.5 Direct Shear Test (DST)**

This laboratory investigation is used to estimate the parameters for soil's shear strength. It is a straightforward and rapid test that could be carried out on cohesive and non-cohesive soils.

The direct shear method is a straightforward and usually employed measure in the geotechnical engineering. For the stability evaluation of slopes, foundations, as well as retaining walls, it is frequently utilised to calculate the shear strength characteristics of soils. The soil's shear strength, cohesion, & internal friction angle are the parameters for the shear strength that is calculated from the measurement. Cohesion quantifies the strength of soil particles, whereas the internal friction angle quantifies the resistance of soil to sliding under shear stress. The shear parameters of the sample of soil were calculated in accordance with the IS:2720 (Part 13)-1986.

The samples were collected by inserting a 60mm x 60mm x 25mm sampling device into the sampler's collected samples. The specimens have been cut and flattened before testing. All of the samples were sheared in a direct shear machine at the rate of 1.25 mm/min. Maximum shear stress values were calculated at normal stress levels of 0.5 kg/cm<sup>2</sup>, 1 kg/cm<sup>2</sup>, & 1.5 kg/cm<sup>2</sup>. Normal stress was then plotted as abscissa along with shear stress as ordinate on a graph between normal stress and maximal shear stress. Intercept of the graph at the Y-axis depicts cohesion (c), & the slope of the line specifies the angle of internal friction ( $\phi$ ).



Figure 4.3 Shows the Direct Shear Test Assembly

## **4.2 Numerical Modelling**

In this research, soil slope is examined with the help of GeoStudio 2020 software. The entire procedure of numerical modelling is conducted in 3 stages. Starting with the first stage, limit equilibrium process-oriented Slope/W tool was employed to evaluate the slope's stability prior to rainfall. Seep/W, a finite element tool, was next employed to simulate the amount of rainfall, and the results were used once more into Slope/W to evaluate stability of the wet slope following heavy rainfall. After that the slopes that were failed after the effect of rainfall were stabilised using geosynthetics of length 23m in three, four, five and six layers.

### **4.2.1 Seepage Analysis During Rainfall**

We can evaluate the pressure created by pore water that is caused by rainfall of suitable intensity based on slope geometry, the specified material property, and the related starting & boundary conditions using 2D finite element method utilising SEEP/W. It works by employing a numerical discretization method to solve Darcy's equation for a particular slope condition and then executing water flow regulating equations to calculate 2D seepage. During the analysis of seepage through SEEP/W which is a FEM (finite element software) (a version of GeoStudio 2020), the flux boundary  $q$  corresponding to intended rainfall duration & intensity is then applied to the slope surface. To avoid excessive rainfall accumulating on the slope surface, a non-ponding boundary condition has been established. The fundamental knowledge required to describe the mechanical behaviour of the unsaturated soil is contained in the soil-water



characteristic curve (SWCC). The SWCC and other related qualities like shear strength and permeability are often described using certain parameters like air-entry value, slope at the inflection point, residual water content, and residual suction (Zhai and Rahardjo, 2012).

The SEEP/W equations depend on Darcy's law as well as the continuity formula for the flow of groundwater.

In general, Darcy's law is as follows:

$$Q = -kA \left( \frac{dh}{dl} \right) \quad (3)$$

where Q represents the flow rate, k represents the hydraulic conductivity linked with soil, A represents the flow path's cross-sectional area, and dh/dl represents the hydraulic gradient.

The equation for continuity for the flow of groundwater is:

$$\frac{d}{dx} \left( \frac{Tdx}{dx} \right) + \frac{d}{dy} \left( \frac{Tdy}{dy} \right) + \frac{d}{dz} \left( \frac{Tdz}{dz} \right) = S \quad (4)$$

where T represents the soil's transmissivity, S represents the source or outlet for the flow of groundwater, and x, y, and z represent the spatial coordinates. SEEP/W employs finite element modelling to discretize the ground water flow models and calculate the hydraulic potential and rate of flow at each mesh node. The software also includes modelling options for boundary conditions, like specified head or flux, and different kinds of soil properties, including anisotropy and heterogeneity.

The principal partial differential equation for a 2-dimensional transient water flow used in the finite element seepage calculation is (Fredlund and Rahardjo, 1993)

$$m_w^2 \gamma_w \frac{\partial h_t}{\partial t} = \frac{\partial}{\partial x} \left( -k_{wx} \frac{\partial h_t}{\partial x} \right) + \frac{\partial}{\partial y} \left( -k_{wy} \frac{\partial h_t}{\partial y} \right) + q \quad (5)$$

where  $m_w^2$  is the slope of the SWCC (soil-water characteristic curve);  $\gamma_w$  is the water unit weight;  $h_t$  is the hydraulic head or total head; and t is the elapsed time; q is applied boundary flux;  $k_{wx}$  permeability coefficient with respect to the water as a result of matric suction in the x direction;  $k_{wy}$  permeability coefficient with respect to the water as an operation of matric suction in the y direction.

Input data, such as soil characteristics and boundary conditions, will be needed for seepage analysis. SWCC (soil water characteristic curve) & HCF (hydraulic conductivity function) necessitate soil property input in the unsaturated or saturated model. The volumetric water content function in GeoStudio is defined by the volumetric data point function, Fredlund-Xing function, Van Genuchten function, and sample function. The volumetric data point function has been selected from among these functions for this investigation. SEEP/W uses two models, Fredlund-Xing and Van Genuchten, as input hydraulic data point functions for predicting

unsaturated hydraulic conductivity. At this instance of SWCC, the saturated hydraulic permeability ( $k_s$ ), volumetric water content ( $s$ ), & residual water content ( $r$ ) must be provided as input parameters for calculation of the unsaturated hydraulic conductivity using the Van Genuchten equation.

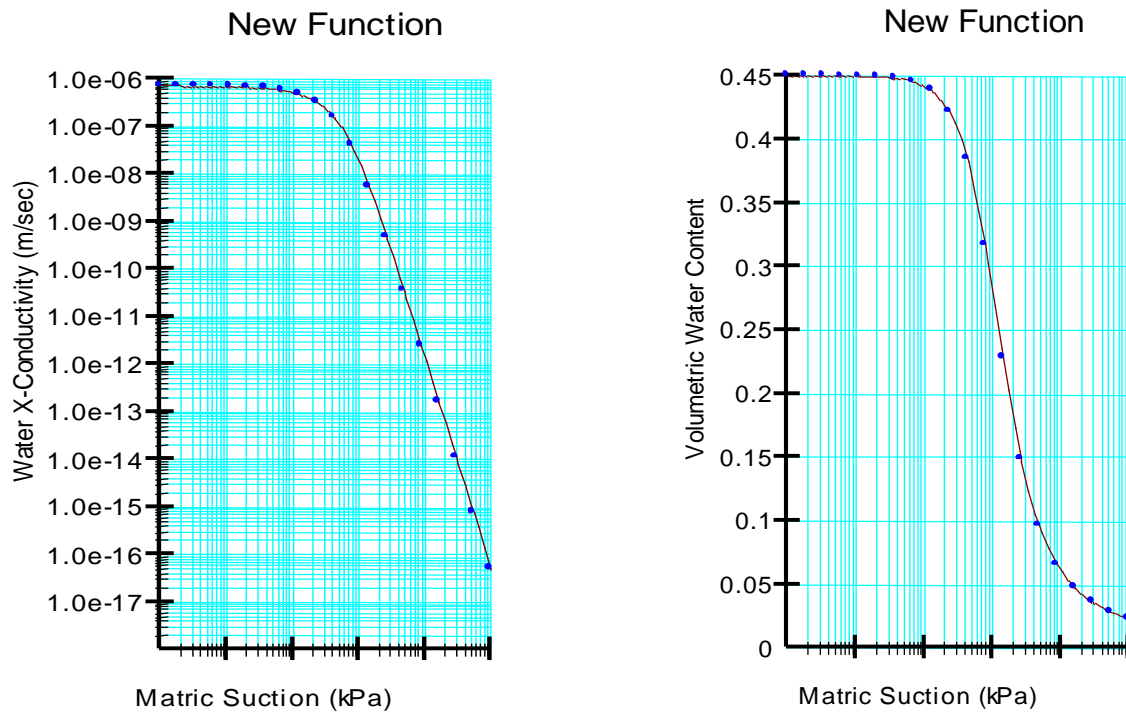


Figure 4.4 HCF and SWCC for study location

#### 4.2.2 Analysis of slope stability using SLOPE/W

Slope/W tool of GeoStudio software, which is focused on the limit equilibrium technique, is employed to assess the stability of slope. Although there are alternative techniques to determine the safety factors of the slopes, we'll be utilising the Morgenstern-Price method in this study. This method is employed due to its advantage of accounting for moment and force balance. The water pressure is negative above the water's surface level on a saturated-unsaturated slope, and this negative water pressure affects the stability and suction of slopes. The Mohr-Coulomb criteria for failure is adjusted as shown in equation 6 to account for the impact of suction just on slopes' resistant shear strength and safety factor.

$$\tau_f = C' + (\sigma_n - u_a)\tan\phi' + (u_a - u_w)\tan\phi^b \quad (6)$$

Where:  $C'$  is the effective cohesion,  $\phi'$  is the internal friction angle,  $u_w$  is sliding surface's pore

pressure,  $\varphi^b$  is saturated zone's internal friction angle,  $u_a$  is sliding surface's pore air pressure. Also  $\varphi' = \varphi^b$ .

From the analysis done in SEEP/W the derived phreatic surfaces were added to the SLOPE/W (GeoStudio 2020), a limit-equilibrium oriented application, in order to conduct the stability, check on the slope having low permeability under different rainfall conditions, with & without the use of geosynthetic. Using a Morgenstern-Price method, the universal safety factor of the slope was computed in these two instances. This method is utilised because it takes moment as well as force balance into account. The function of reinforcement in the geosynthetics was accounted in SLOPE/W by providing the value of bond skin friction (kPa) & tensile capacity (kN/m) of the layers of geosynthetic (as stated in Table 3.1) in the analysis as the input parameters. The input parameters for reinforcement loads is depicted in Figure 4.5.

R..	Type	X Outside Pt (...)	Y Outside Pt (m)	X Inside Pt (m)	Y Inside Pt (m)	Length (m)	Dire...
1	Geosynthetic	86.83	76.5	63.83	76.5	23	0
2	Geosynthetic	92.66	72	69.66	72	23	0
3	Geosynthetic	98.49	67.5	75.49	67.5	23	0
4	Geosynthetic	104.33	63	81.33	63	23	0
5	Geosynthetic	110.16	58.5	87.16	58.5	23	0

1 Geosynthetic 86.83 m 76.5 m 63.83 m 76.5 m 23 m 0°

F of S Dependent: No Force Distribution: Distributed Face Anchorage: Yes

Pullout Resistance (F/Area): 12.5 kPa Tensile Capacity: 55.35 kN

Calculate Pullout Resistance from: Reduction Factor: 1.5

Interface Adhesion: 0 kPa Force Orientation: 0 (0 - Axial, 1 - Parallel to Slice Base)

Interface Shear Angle: 0°

Surface Area Factor: 2

Resistance Reduction Factor: 1.5

Figure 4.5 Input parameters for reinforcement loads

## CHAPTER 5 RESULTS AND DISCUSSIONS

### 5.1 Experimental Results

#### 5.1.1 Particle Size Distribution Analysis

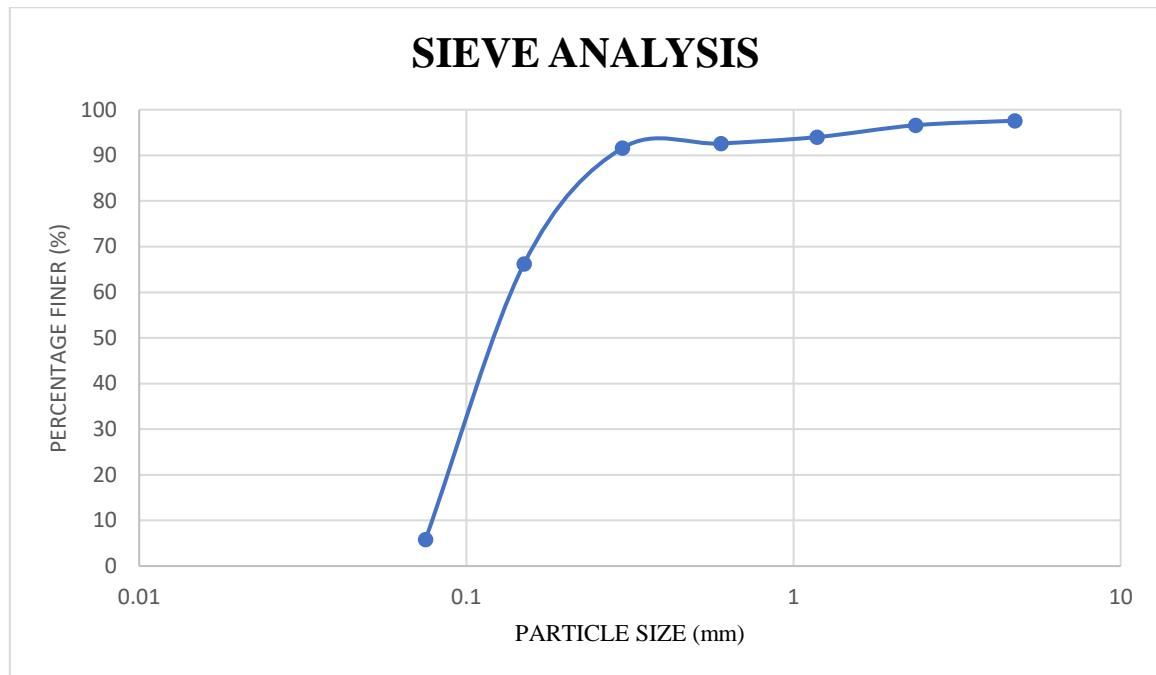


Figure 5.1 Particle size distribution curve

Table 5.1: Uniformity Coefficient and Curvature Coefficient of soil sample

Parameters	Values
<b>D<sub>10</sub> (mm)</b>	0.1445
<b>D<sub>30</sub> (mm)</b>	0.4756
<b>D<sub>60</sub> (mm)</b>	0.9723
<b>Uniformity Coefficient</b> $C_u = D_{60} / D_{10}$	<b>6.7273</b>
<b>Curvature Coefficient</b> $C_c = D_{30}^2 / (D_{10} \cdot D_{60})$	<b>1.6098</b>

### 5.1.2 Specific Gravity Test

Table 5.2 Specific Gravity of soil

		Sample 1	Sample 2	Sample 3
Mass of empty Pycnometer	M <sub>1</sub> (gm)	698	698	698
Empty Pycnometer + Dry Soil	M <sub>2</sub> (gm)	798	798	798
Empty Pycnometer + Dry Soil +Water	M <sub>3</sub> (gm)	1632	1636	1634
Empty Pycnometer +Water	M <sub>4</sub> (gm)	1572	1572	1572
Specific Gravity	G	2.50	2.77	2.63

Average value of specific gravity of Soil sample =  $(2.50 + 2.77 + 2.63)/3 = 2.63$

### 5.1.3 Atterberg Limits Test

Table 5.3 Atterberg Limits

S.No	Parameters	Values
1.	Liquid Limit (%)	31
2.	Plastic Limit (%)	21.24
3.	Plasticity Index (%)	9.76

In this research, value of curvature coefficient ( $C_c$ ) and uniformity coefficient ( $C_u$ ) came out to be 1.6098 and 6.7273. As value of  $C_c$  is between 1 & 3, and value of  $C_u$  is larger than 6. Also, the percentage of sample of soil passing from 4.75 mm sieve is greater than 50%. Therefore, the sample of soil is well graded sand (SW) and as liquid limit is less than 35% the soil is low plastic in nature and soil contains some proportion of clay and some proportion of silt.

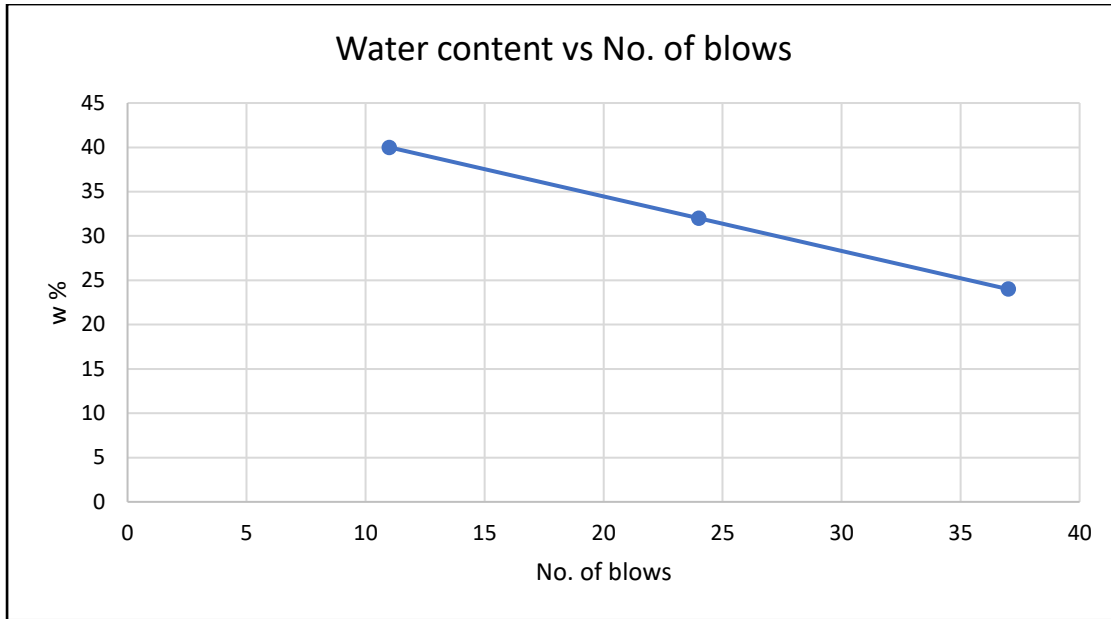


Figure 5.2 Variation of water content with No. of blows

#### 5.1.4 Compaction Test

Table 5.4 Water Content and Dry Density relation for compaction test

S. NO.	DRY DENSITY, $\gamma_d$ (kN/m <sup>3</sup> )	WATER CONTENT, w (%)
1	11.20	7.48
2	13.66	10.83
3	11.48	15.74

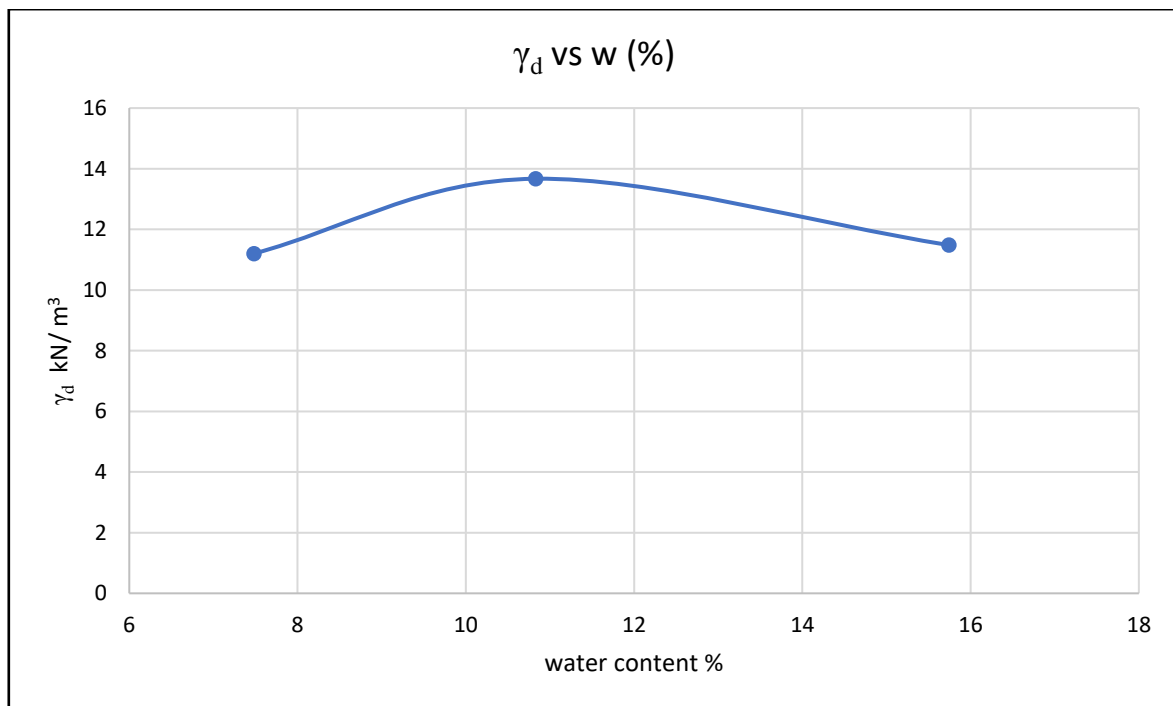


Figure 5.3 Variation of Dry density with water content

Table 5.5 Results of Compaction test

	OMC (%)	MDD, $\gamma_{dmax}$		Corresponding Bulk density, $\gamma_b$	
		(g/cm <sup>3</sup> )	(kN/m <sup>3</sup> )	(g/cm <sup>3</sup> )	(kN/m <sup>3</sup> )
Soil sample	10.83	1.392	13.66	1.544	15.15

### 5.1.5 Direct Shear Test

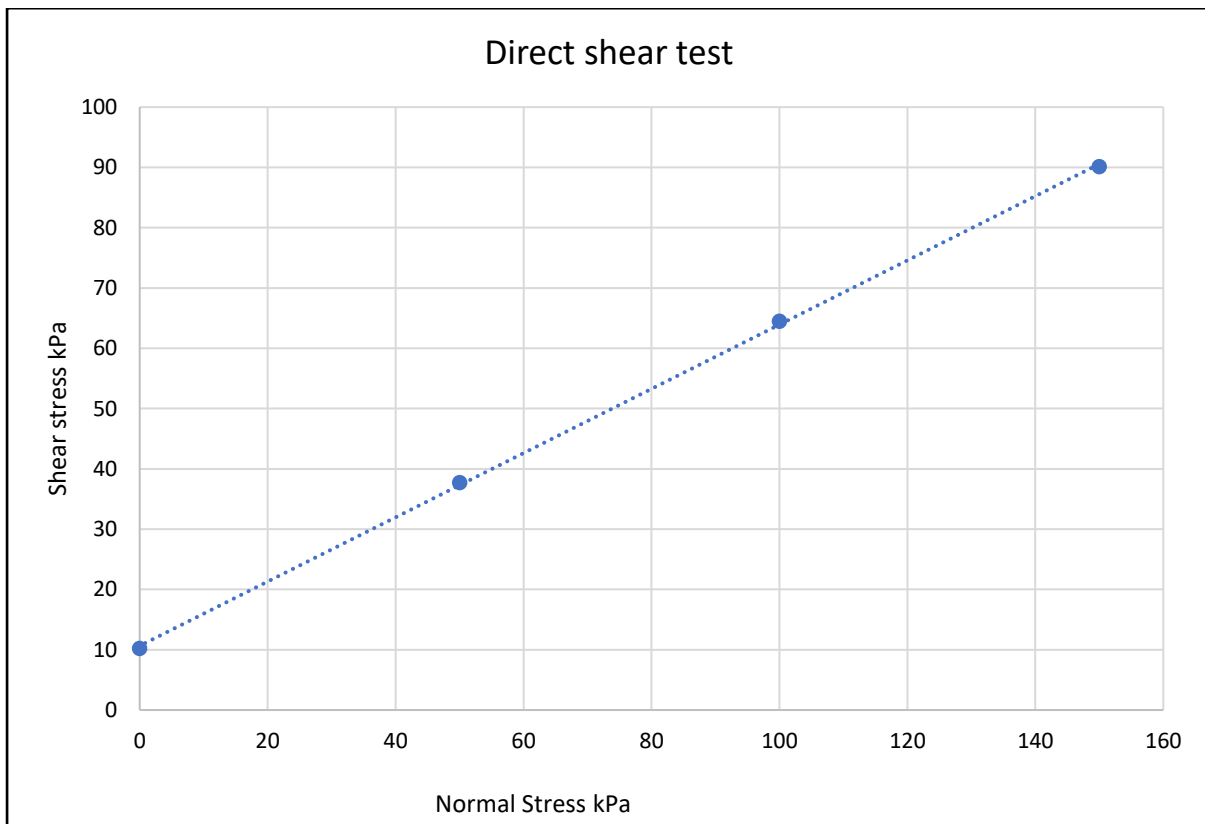


Figure 5.4 Mohr- Coulomb Failure envelope

Table 5.6 Values of cohesion (c) and internal friction angle ( $\phi$ )

Cohesion (g/cm <sup>2</sup> )	10.21
Internal Friction Angle (°)	30.5

Table 5.7 Showing values of different soil properties

S.No.	Soil Property	Values
1.	Natural Water content (%)	5.8
2.	Bulk Unit Weight ( $\gamma_b$ ) (kN/m <sup>3</sup> )	15.15
3.	Dry Unit Weight ( $\gamma_d$ ) (kN/m <sup>3</sup> )	13.66
4.	Saturated Unit Weight ( $\gamma_{sat}$ ) (kN/m <sup>3</sup> )	18.28
5.	Coefficient of permeability (m/hr)	0.0026
6.	Cohesion (Kg/cm <sup>2</sup> )	10.21
7.	Angle of internal friction ( $\varphi^\circ$ )	30.5
8.	Liquid Limit (%)	31
9.	Plastic Limit (%)	21.24

## 5.2 Numerical Modelling

### 5.2.1 Without Geosynthetics

The slopes with slope angle 29.36°, 37.65° and 42° were evaluated for slope stability with before rainfall conditions and after rainfall conditions at max. rainfall, min. rainfall and avg. rainfall.

#### 5.2.1.1 Before Rainfall

The slope's stability is assessed by looking at the unsaturated soil slope before rainfall. The unsaturated slope's safety factor before rainfall turned out to be higher than 1, which supports the slope's stability on its own. Additionally, the research provides the critical slide failure surfaces that could be affected by outside sources. By offering proper stabilisation methods, the critical slip surface can be utilized as preventative measures for design objectives to avert any future failure. Slope stability of three slopes i.e., mild slope, actual slope and critical slope having slope angle 29.36°, 37.65° and 42° respectively were estimated which are shown in Figure 5.5, 5.6 and 5.7.



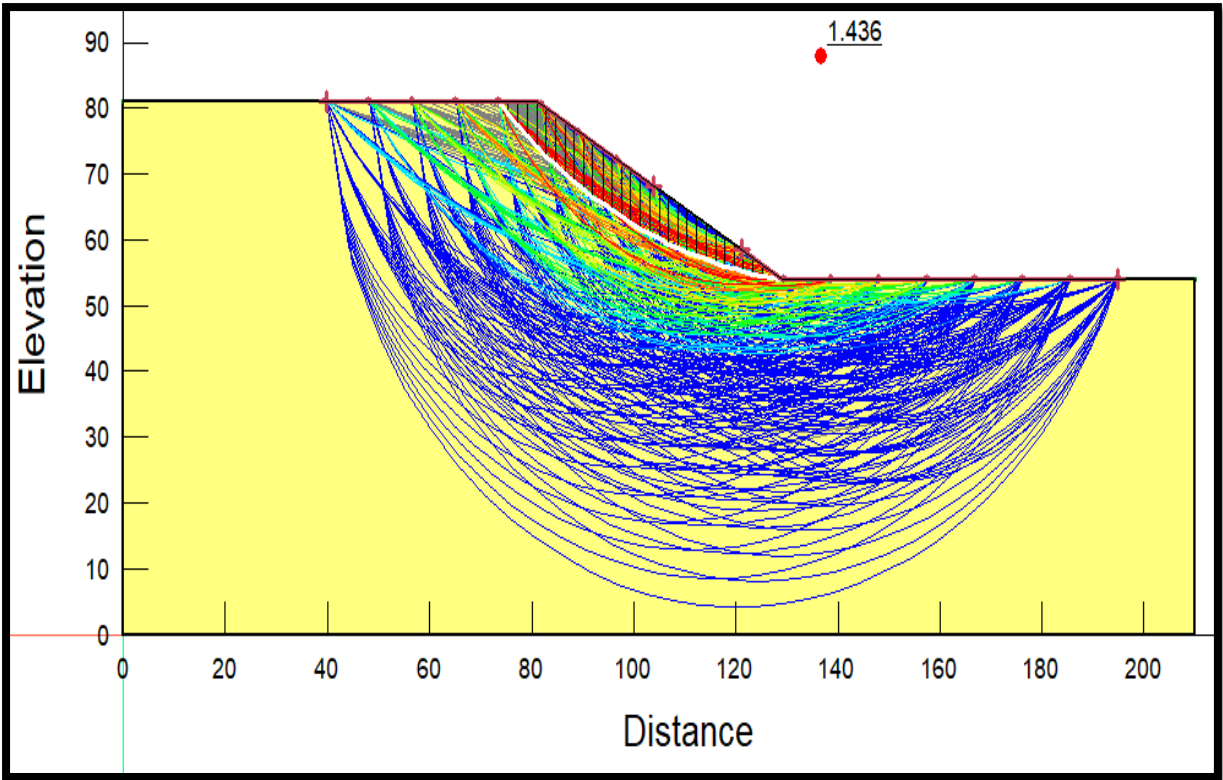


Figure 5.5 For slope with slope angle  $29.36^\circ$  F.O.S is more than 1 before rainfall

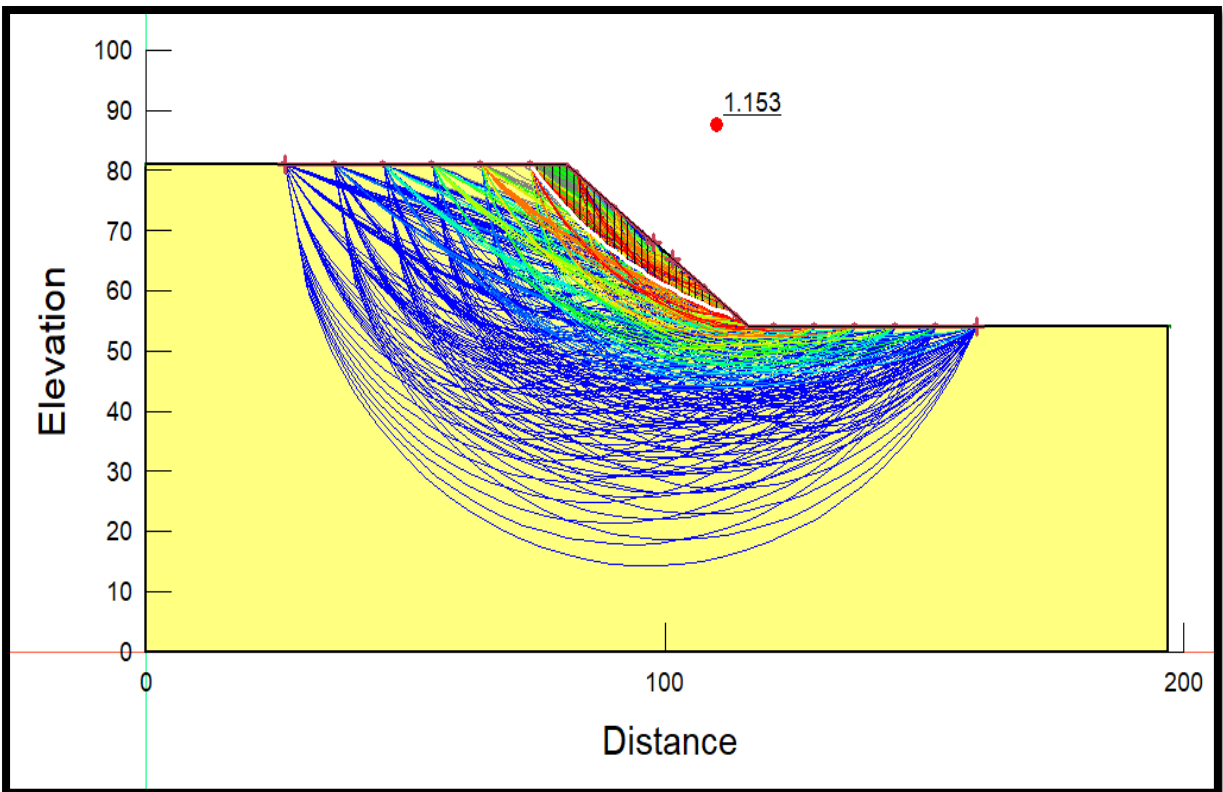


Figure 5.6 For slope with slope angle  $37.65^\circ$  F.O.S is more than 1 before rainfall

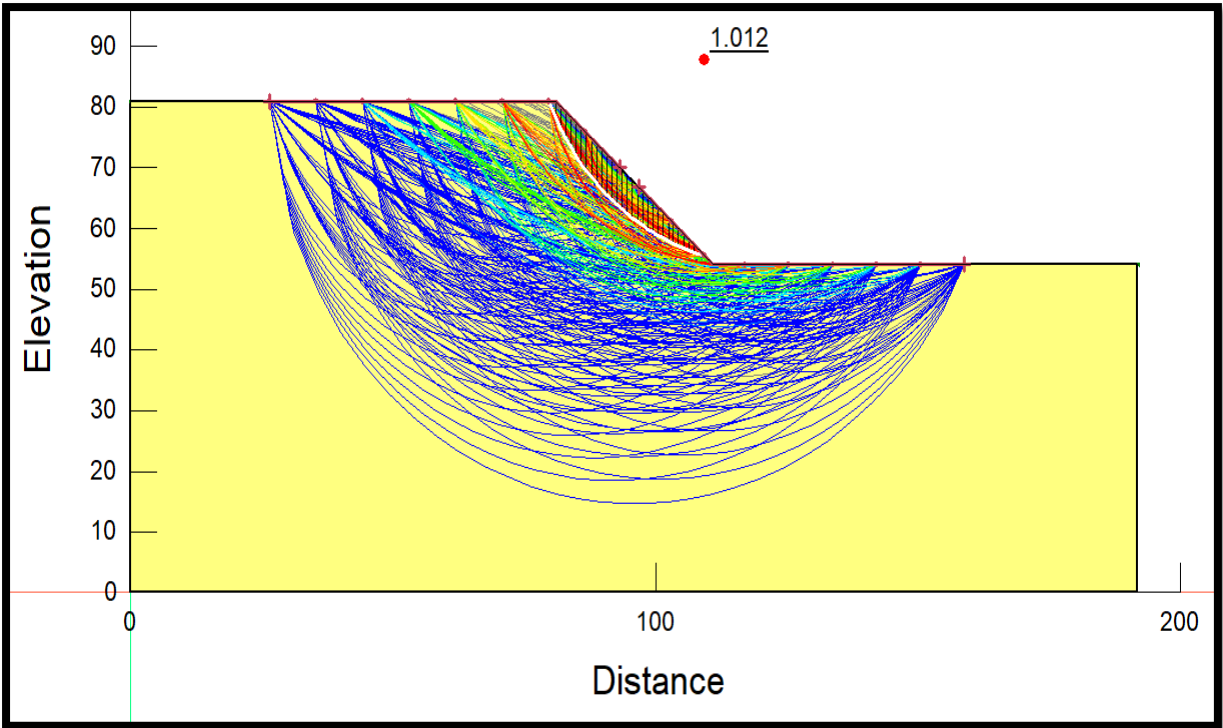


Figure 5.7 For slope with slope angle  $42^\circ$  F.O.S is more than 1 before rainfall

A plot of shear resistance and mobilised shear is shown in Figure 5.8 prior to the inclusion of rainfall intensity on the slope model. As can be seen, that the value of shear resistance is higher than the value of shear mobilised, indicating that the number of forces involved in slope instability is less than the value of forces assisting in slope stability. As a result, our slope is stable prior to rainfall.

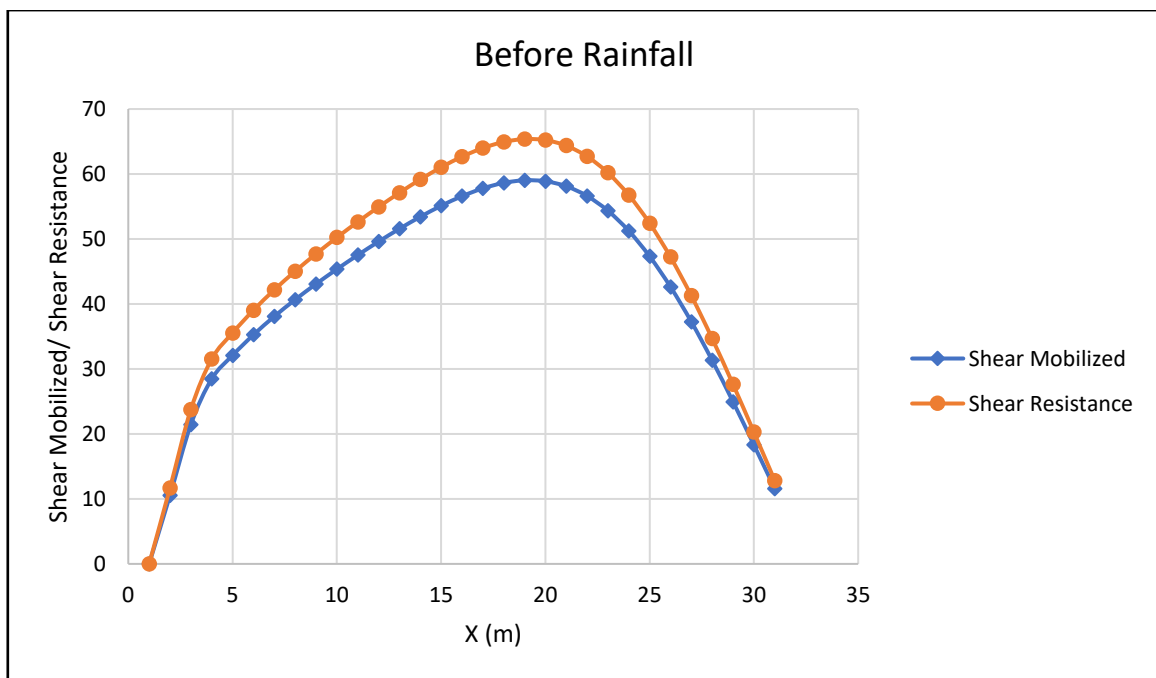


Figure 5.8 Shear Mobilized vs Shear Resistance for slope angle  $37.65^\circ$  before rainfall

### 5.2.1.2 After Rainfall

Now, the study is conducted with various rainfall intensities (max. rainfall, min. rainfall and average rainfall) & boundary conditions for different slopes at different slope angles to track changes in safety factor brought by rainwater infiltration, this is completed in two steps; firstly, analysis of seepage is done using the Seep/W tool, after which the results are utilised to assess the stability of slopes using Slope/W tool. Figure 5.9 to 5.17 depicts the safety factor for the slope at various rainfall intensities, and it is clear from these that the F.O.S. decreases as the intensity of the rainfall rises.

The F.O.S of mild slope which was  $29.36^\circ$  at maximum rainfall, minimum rainfall and average rainfall came out to be 1.207, 1.362 and 1.178 respectively. The F.O.S of actual slope which was  $37.65^\circ$  at maximum rainfall, minimum rainfall and average rainfall came out to be 0.992, 1.085 and 1.137 respectively. The F.O.S of critical slope which was  $42^\circ$  at maximum rainfall, minimum rainfall and average rainfall came out to be 0.928, 1.011 and 1.015 respectively.

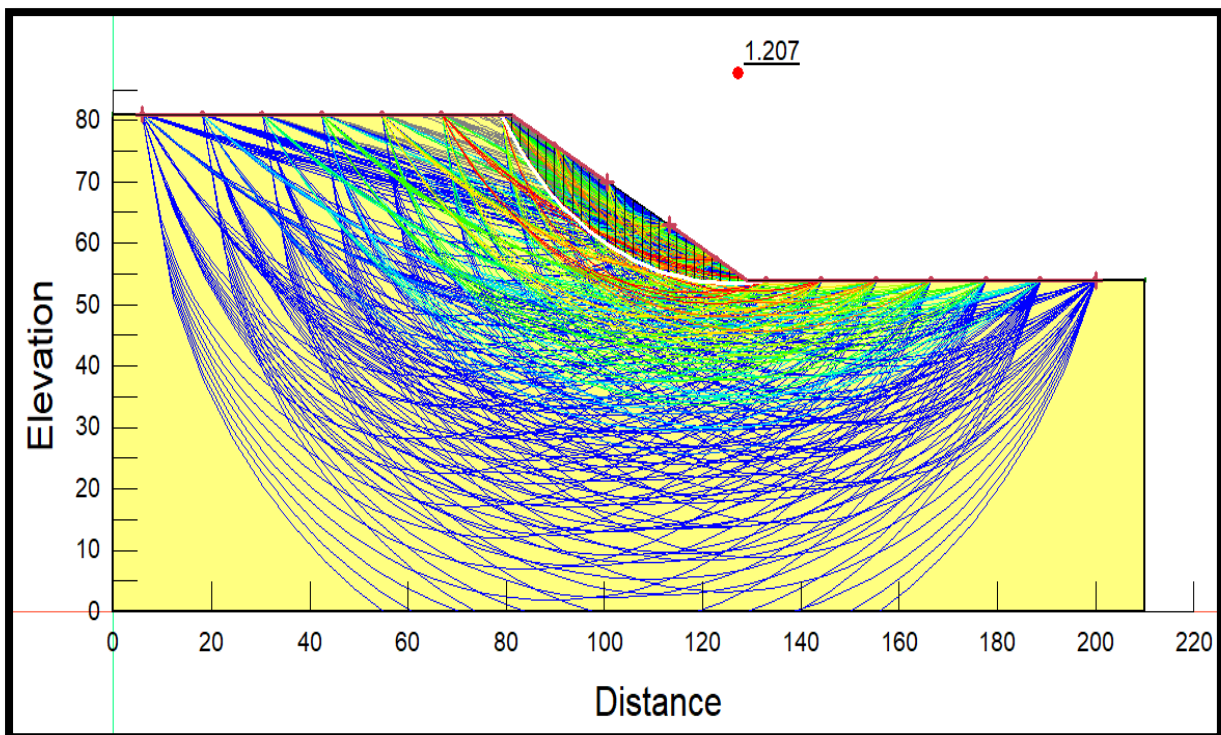


Figure 5.9 For slope angle  $29.36^\circ$  F.O.S is 1.207 at max. rainfall

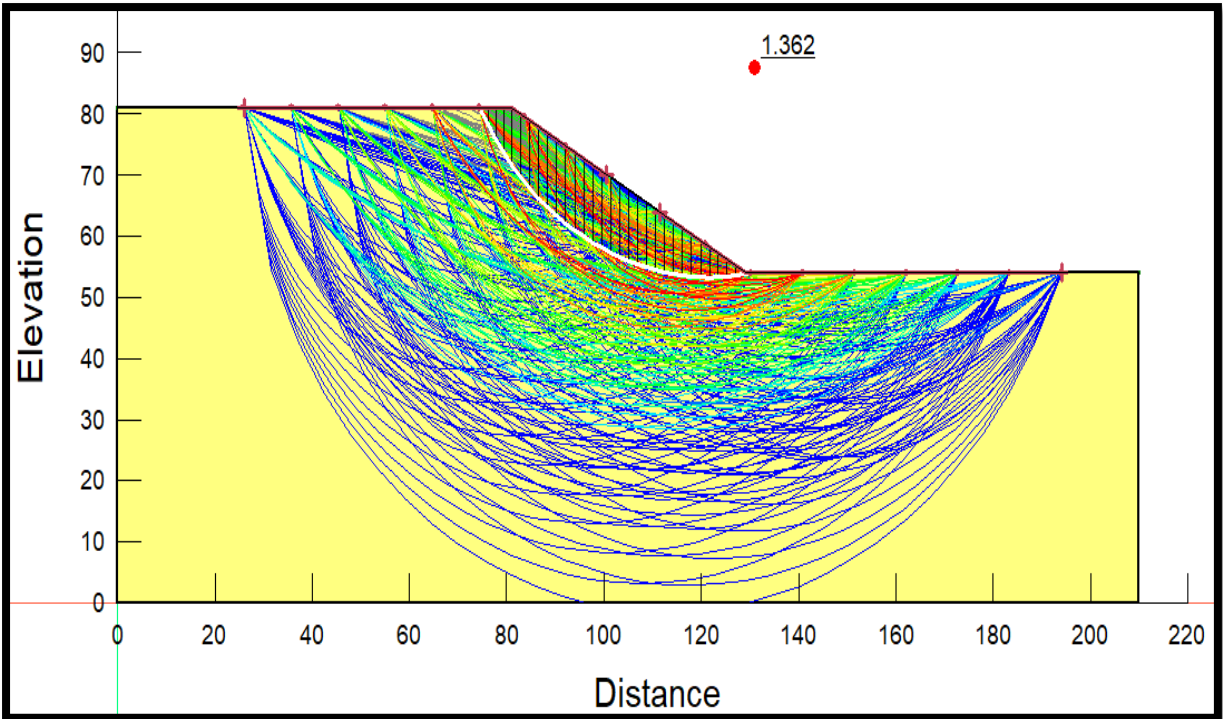


Figure 5.10 For slope angle  $29.36^\circ$  F.O.S is 1.362 at min. rainfall

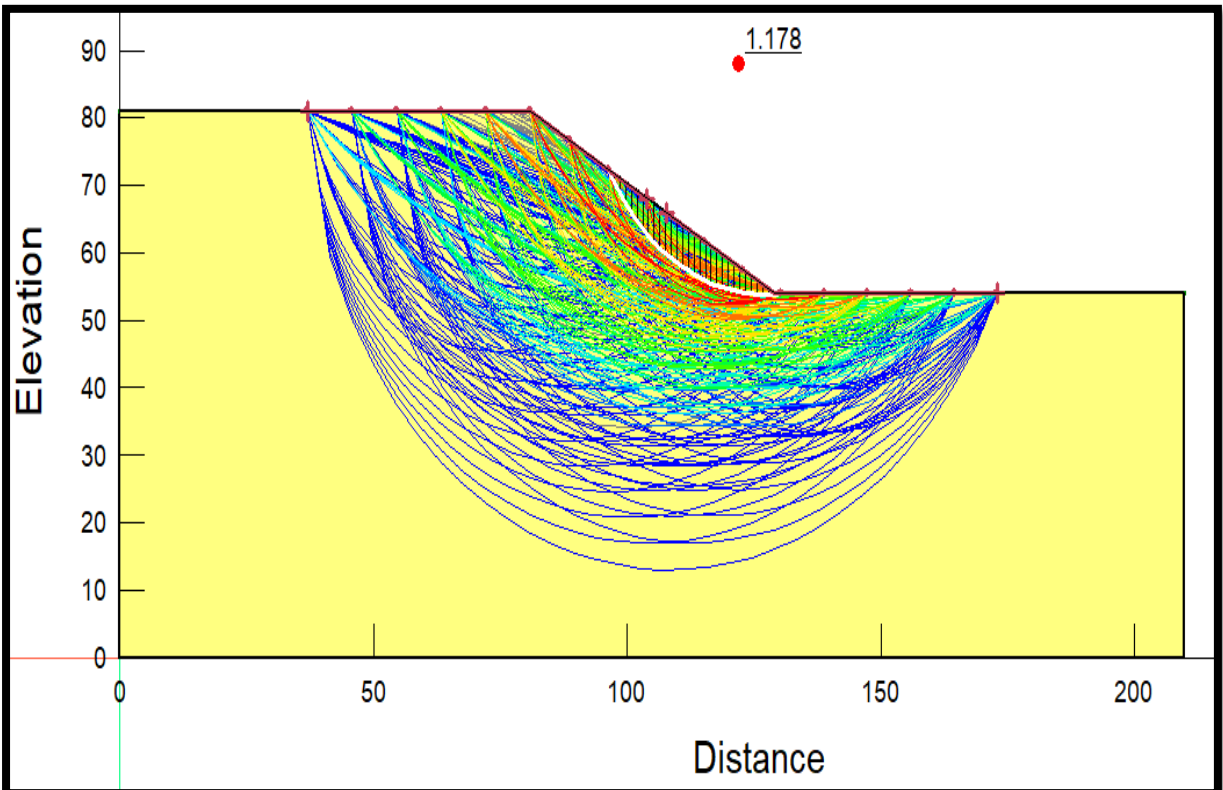


Figure 5.11 For slope angle  $29.36^\circ$  F.O.S is 1.178 at avg. rainfall

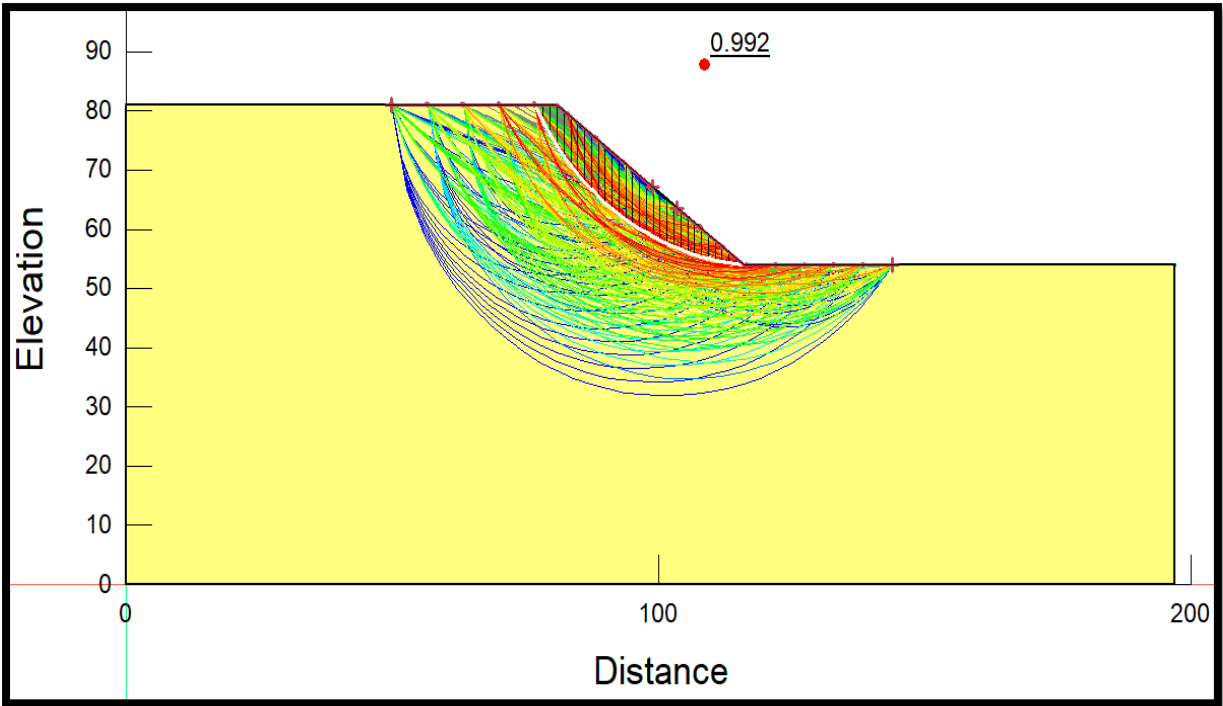


Figure 5.12 For slope angle  $37.65^\circ$  F.O.S is 0.992 at max. rainfall

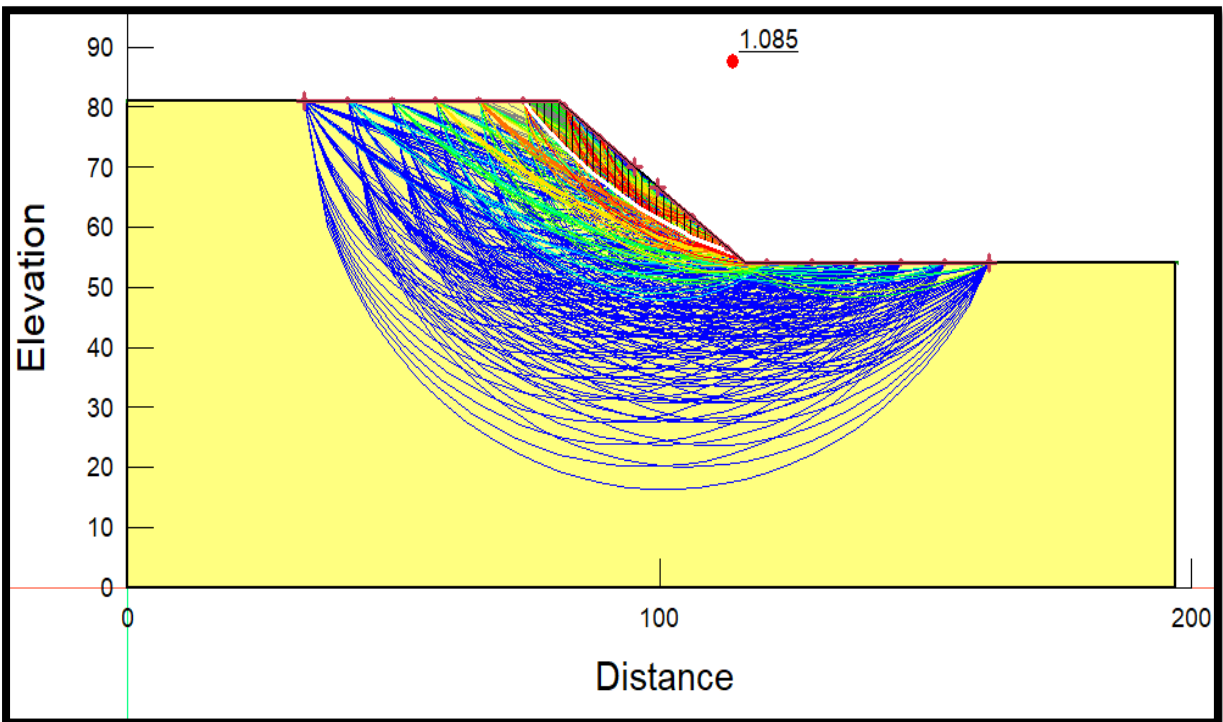


Figure 5.13 For slope angle  $37.65^\circ$  F.O.S is 1.085 at min. rainfall

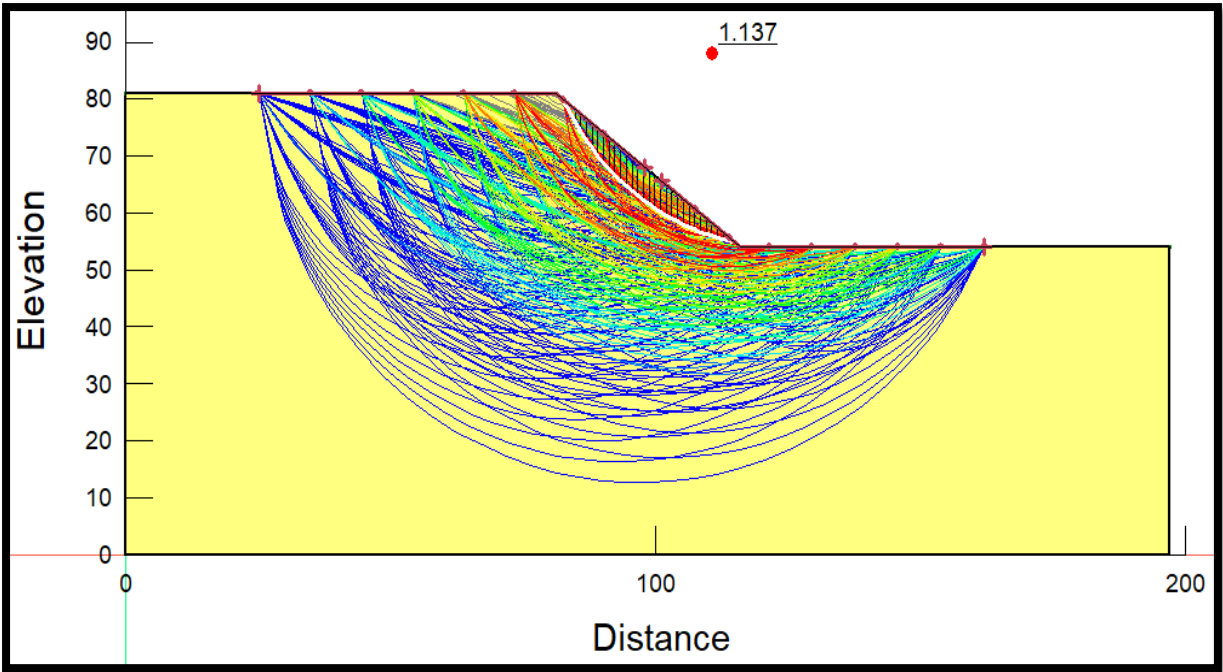


Figure 5.14 For slope angle  $37.65^\circ$  F.O.S is 1.137 at avg. rainfall

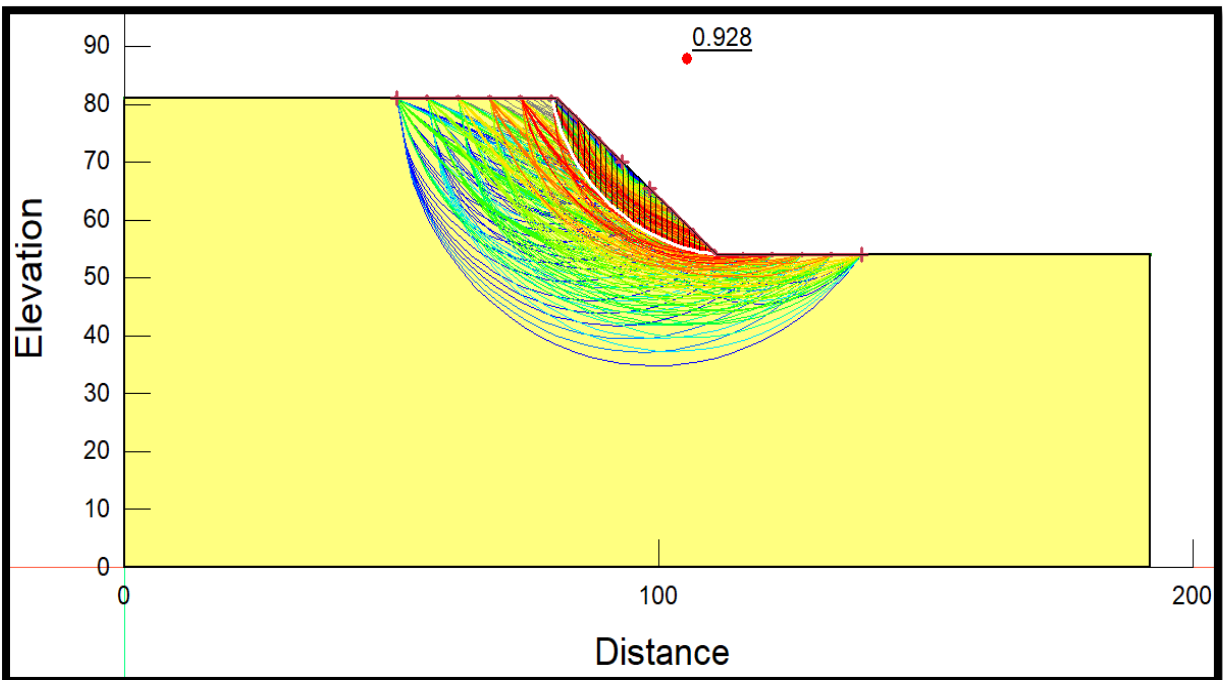


Figure 5.15 For slope angle  $42^\circ$  F.O.S is 0.928 at max. rainfall

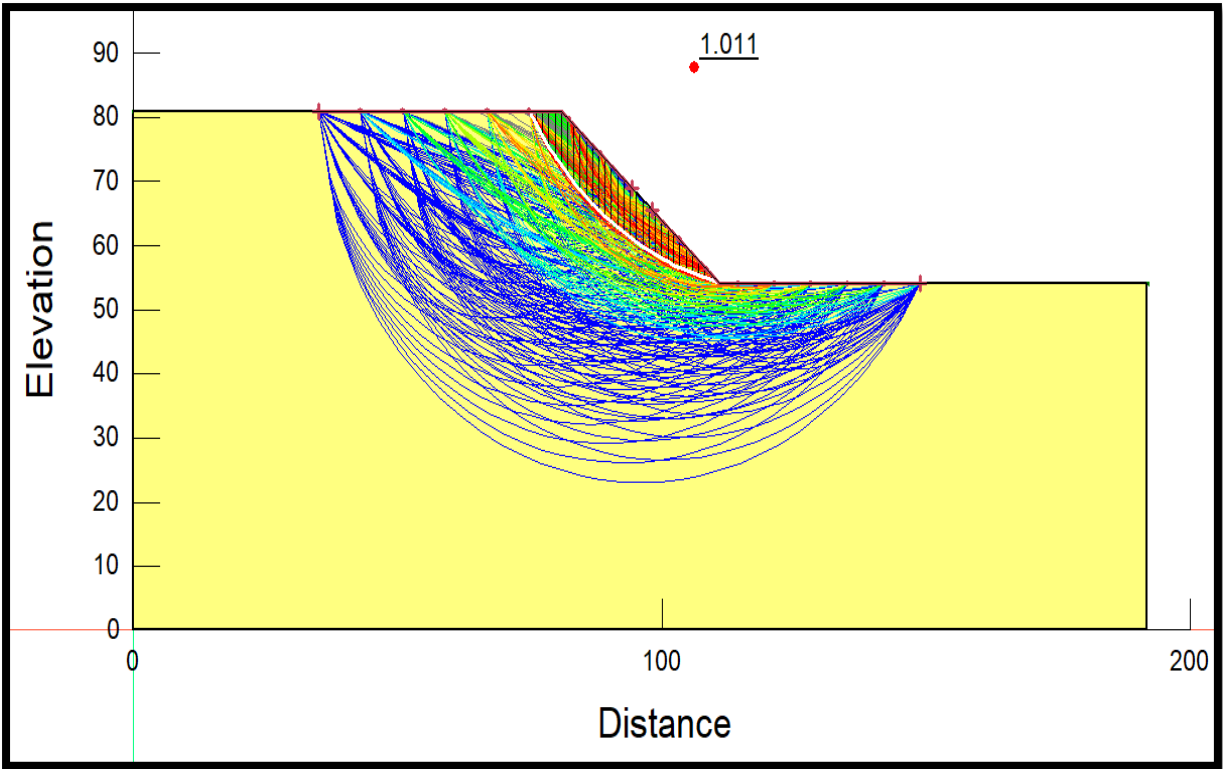


Figure 5.16 For slope angle  $42^\circ$  F.O.S is 1.011 at min. rainfall

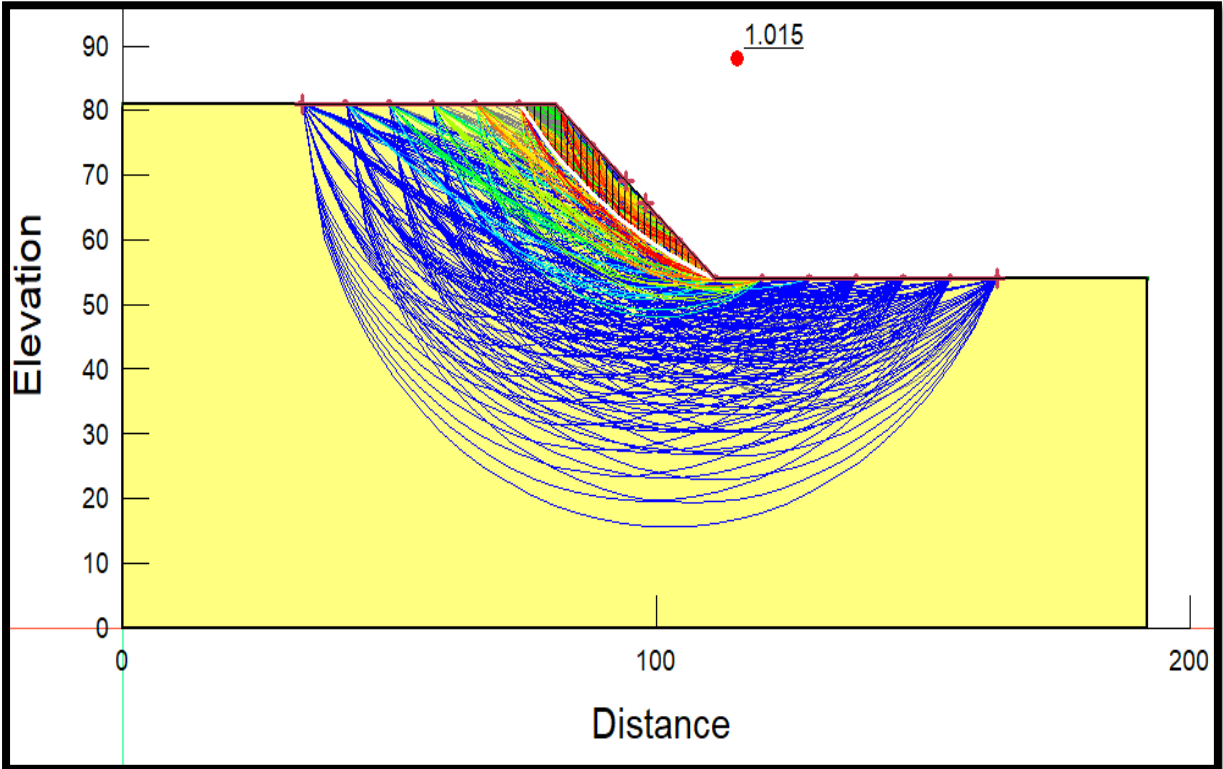


Figure 5.17 For slope angle  $42^\circ$  F.O.S is 1.015 at avg. rainfall

A plot of shear mobilised and shear resistance is shown in Figure 5.18 after the slope model's maximum rainfall intensity has been implemented. As can be seen, that the value of shear mobilised is now higher than the value of shear resistance, indicating that the value of forces involved in slope failure is higher than the value of forces involved in the stability of the slope before the slope fails. Figure 5.19 shows the comparison between slope angle and F.O.S at max. rainfall, min. rainfall and avg. rainfall.

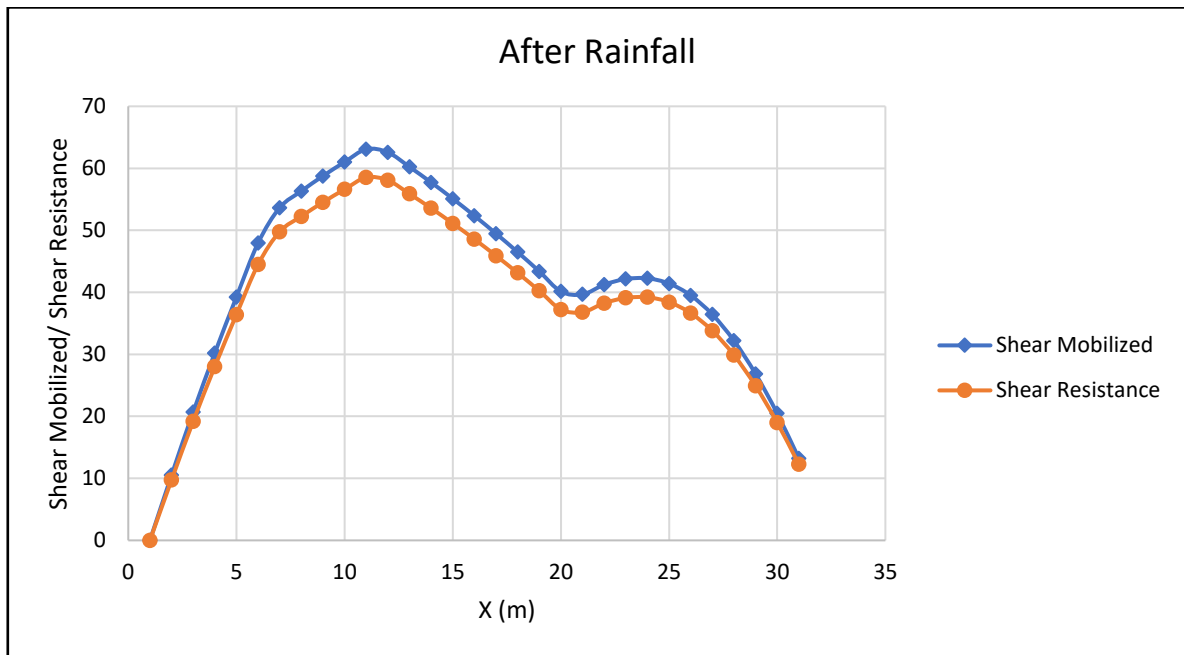


Figure 5.18 Shear Mobilized vs Shear Resistance for slope angle 37.65° after rainfall

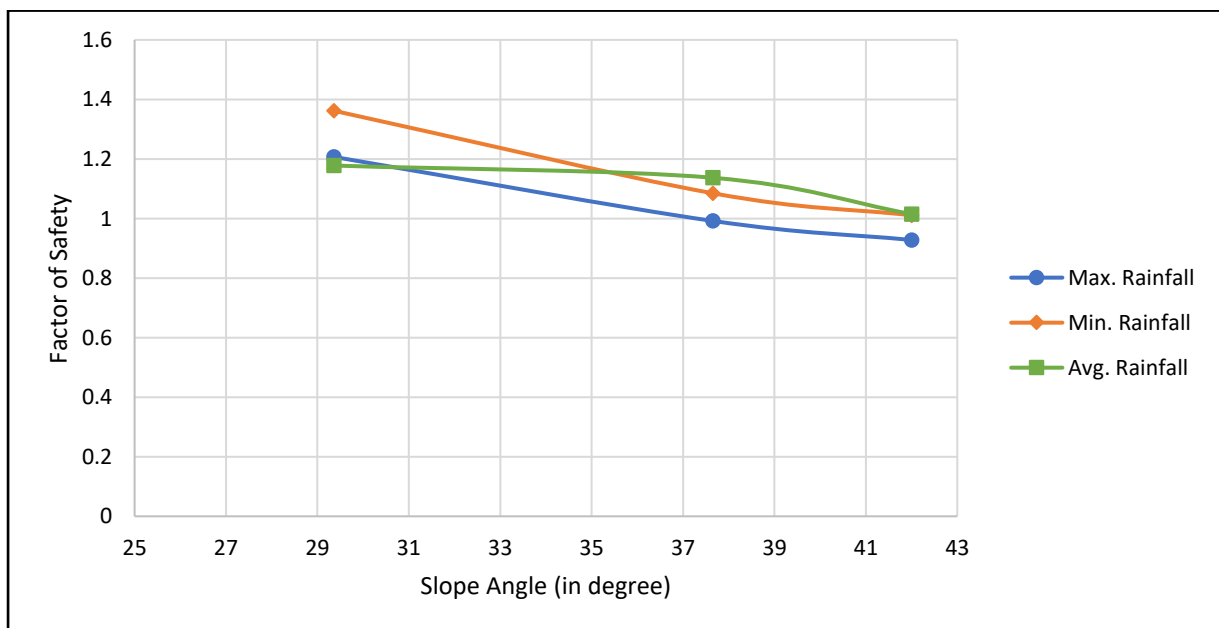


Figure 5.19 Comparison between slope angle and factor of safety at different rainfall intensities



## 5.2.2 With Geosynthetics

### 5.2.2.1 After Rainfall

Two slopes (actual slope with slope angle  $37.65^\circ$  and critical slope with slope angle  $42^\circ$ ) that were failed at maximum rainfall intensity as their factor of safety were 0.992 and 0.928 respectively. The effect of incorporating geosynthetics into a low-permeable slope was investigated by introducing 3, 4, 5, and 6 layers of geosynthetics of length 23 m (which is calculated as 0.85 times the slope's vertical height) (Vishwanadham and Bhattacharjee, 2016). By using the geosynthetics the F.O.S came out to be higher than 1 indicating the stable slope. Figure 5.20 to 5.23 depicts the safety factor for the slope angle  $37.65^\circ$  with 3,4,5 and 6 layers of geosynthetics. Figure 5.24 to 5.27 depicts the safety factor for the slope angle  $42^\circ$  with 3,4,5 and 6 layers of geosynthetics.

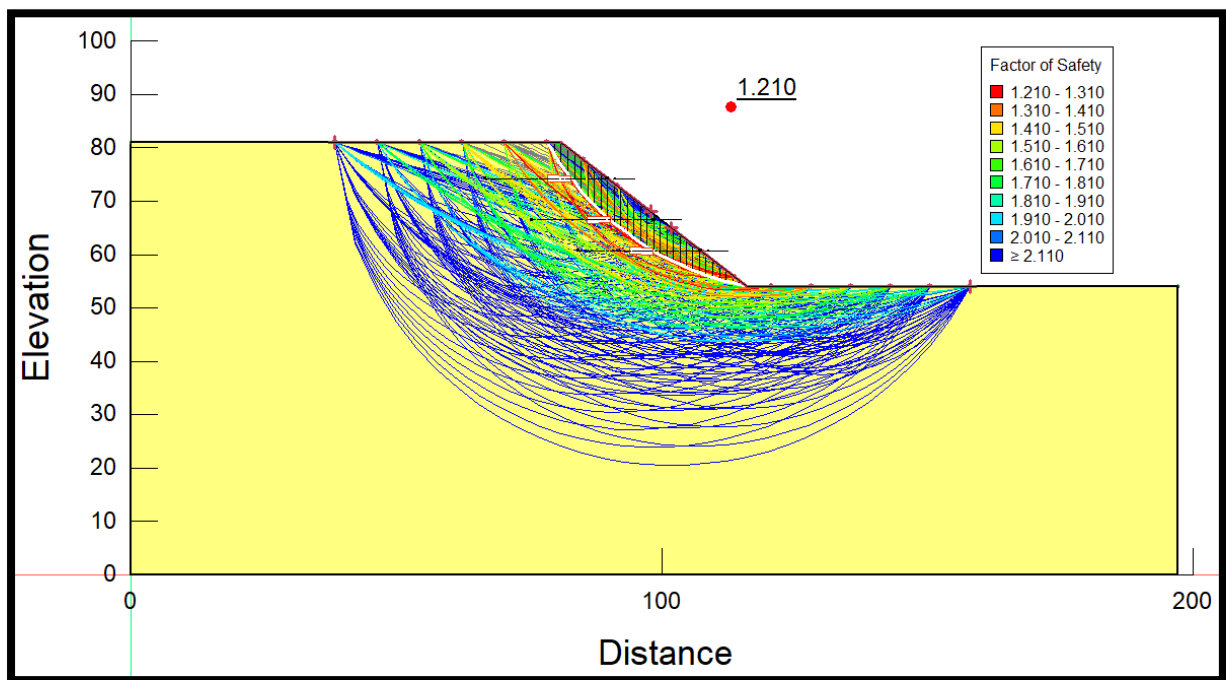


Figure 5.20 For slope angle  $37.65^\circ$  F.O.S is 1.210 with 3 layers of geosynthetic

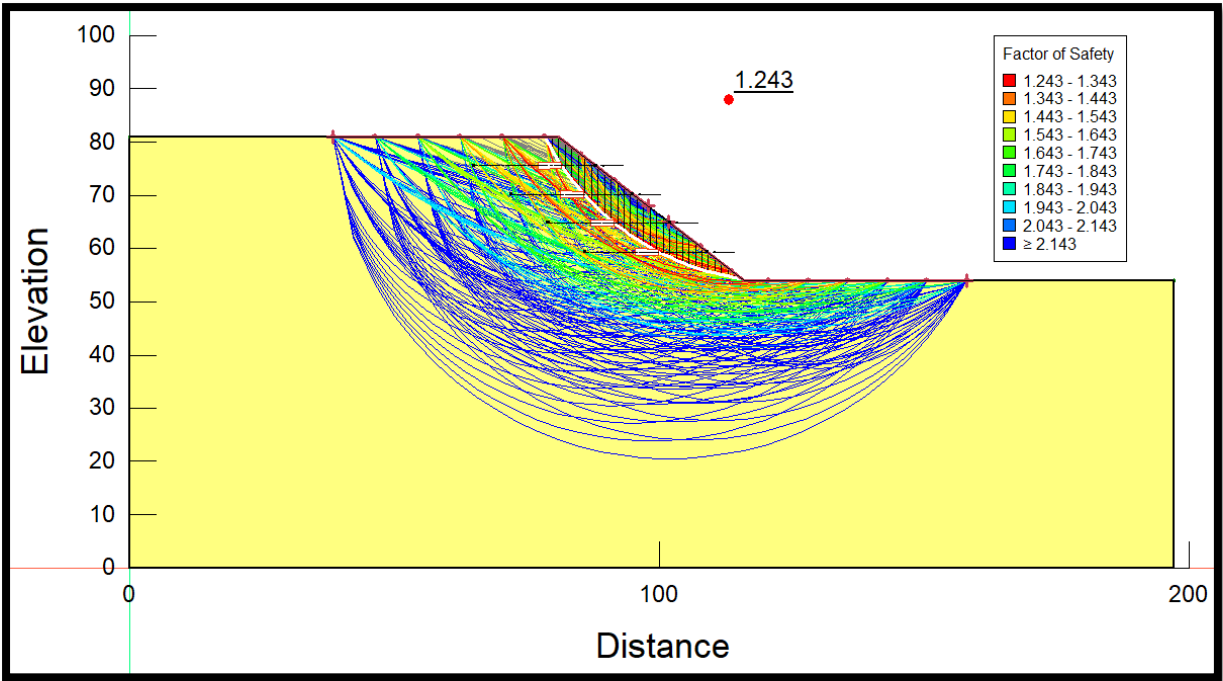


Figure 5.21 For slope angle  $37.65^\circ$  F.O.S is 1.243 with 4 layers of geosynthetic

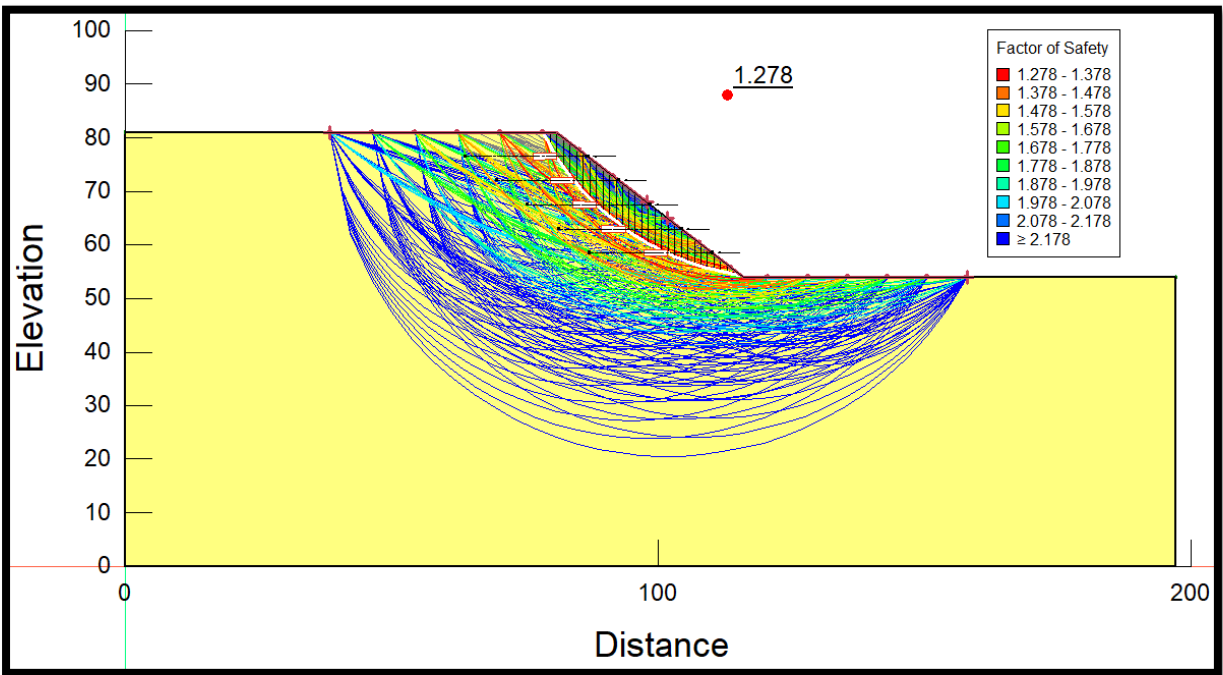


Figure 5.22 For slope angle  $37.65^\circ$  F.O.S is 1.278 with 5 layers of geosynthetic

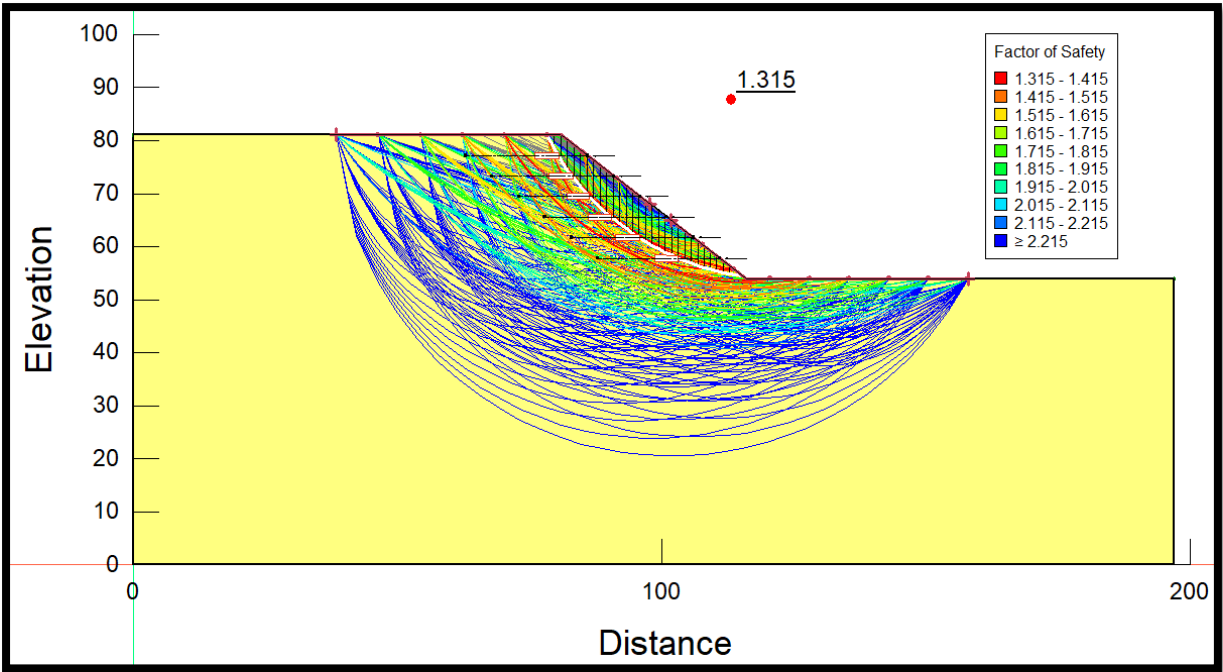


Figure 5.23 For slope angle  $37.65^\circ$  F.O.S is 1.315 with 6 layers of geosynthetic

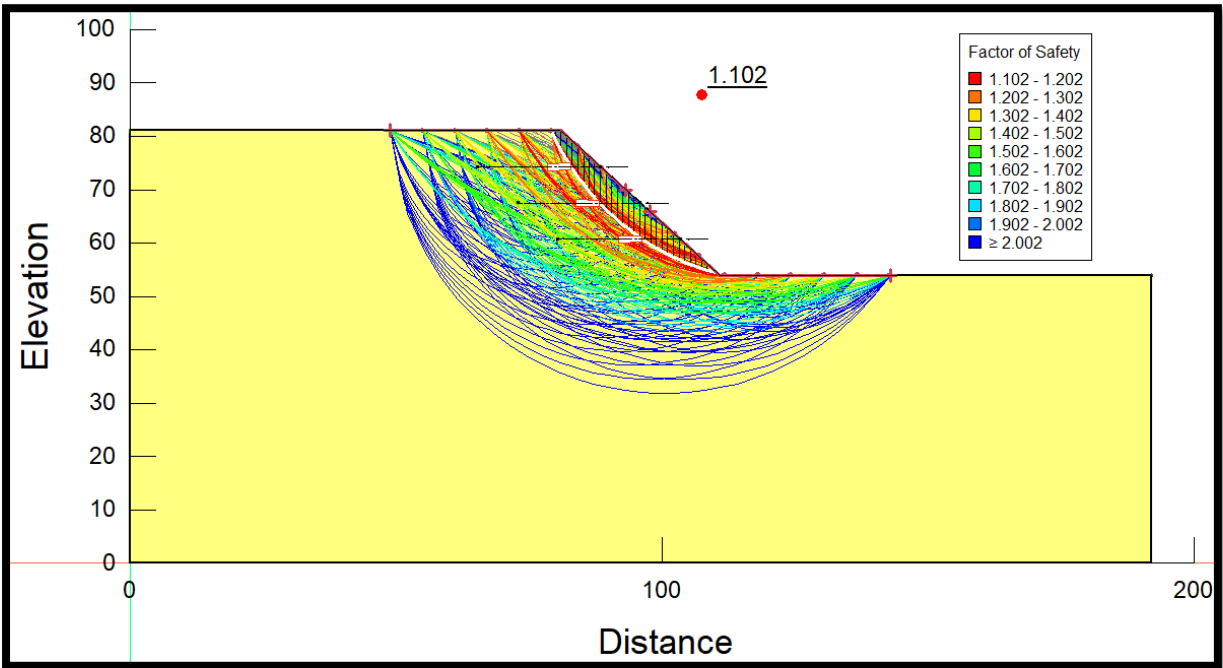


Figure 5.24 For slope angle  $42^\circ$  F.O.S is 1.102 with 3 layers of geosynthetic

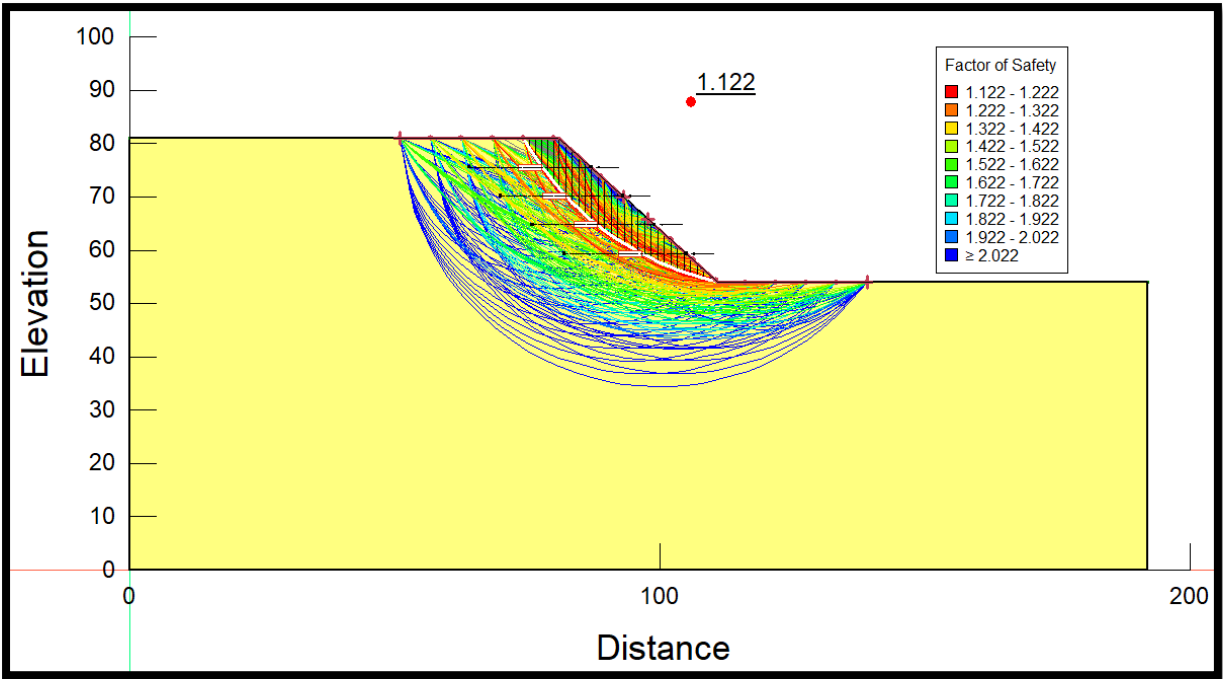


Figure 5.25 For slope angle  $42^\circ$  F.O.S is 1.122 with 4 layers of geosynthetic

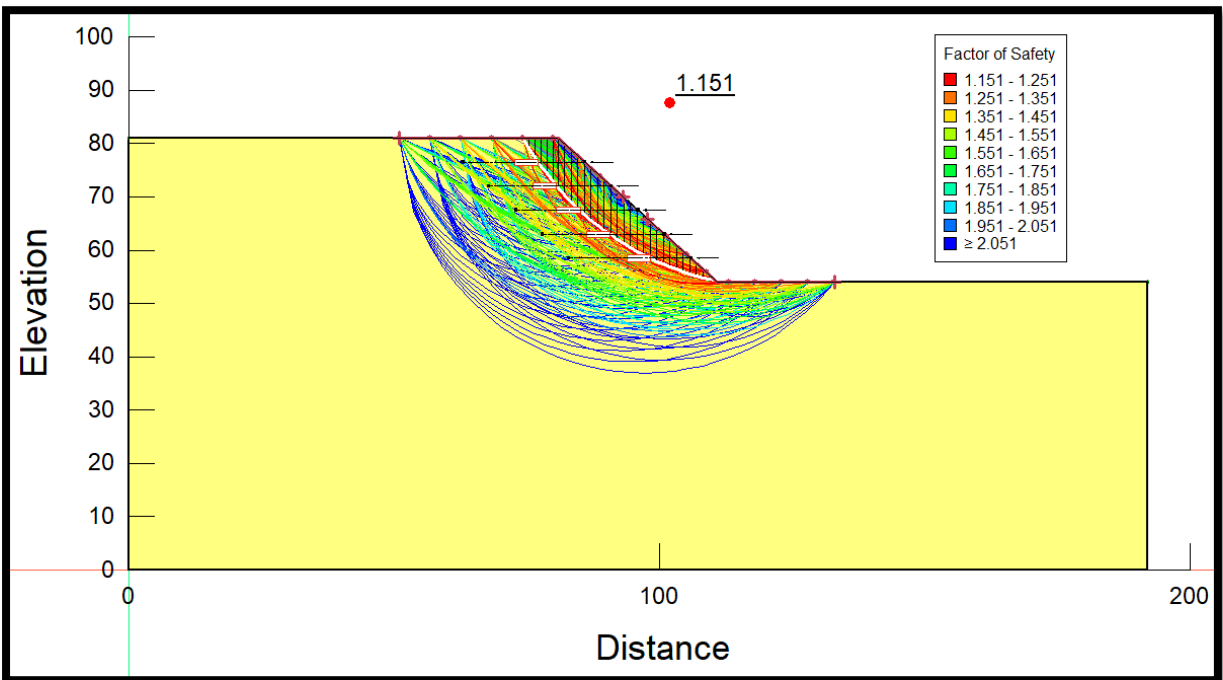


Figure 5.26 For slope angle  $42^\circ$  F.O.S is 1.151 with 5 layers of geosynthetic

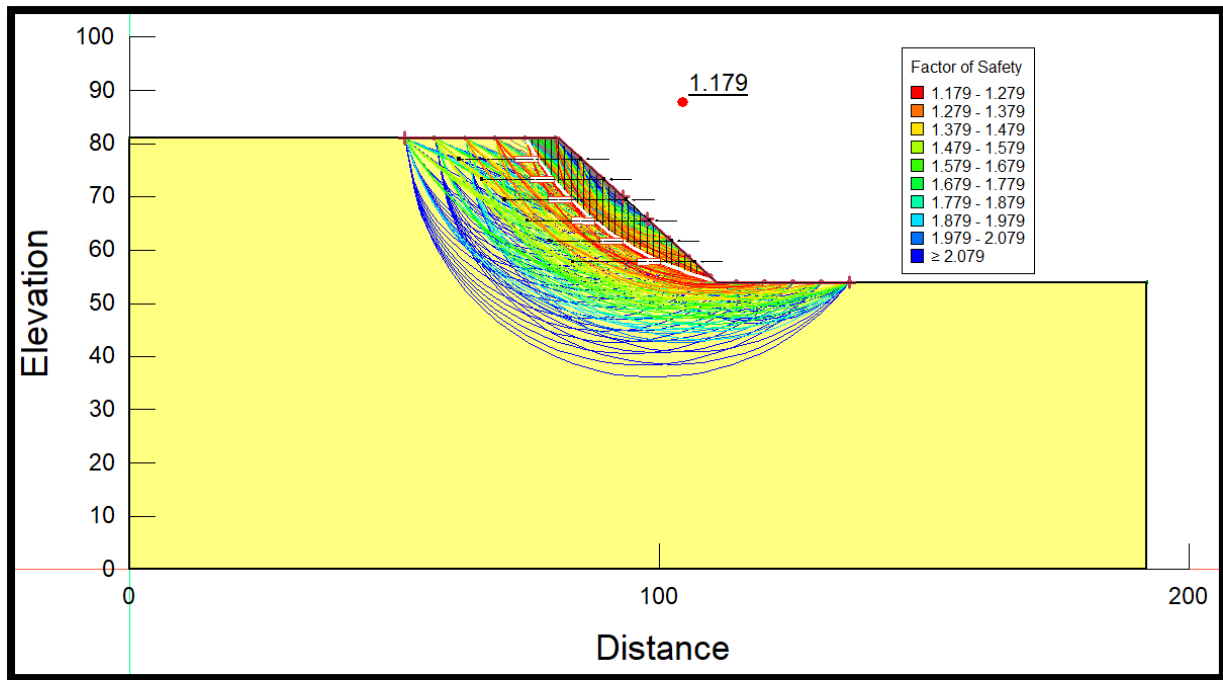


Figure 5.27 For slope angle  $42^\circ$  F.O.S is 1.179 with 6 layers of geosynthetic

### 5.3 Discussions

This study has used numerical evaluation to investigate the process of failure and the impact of rainfall percolation. A steady slope was indicated by a factor of safety before precipitation or pre-monsoon that was greater than 1 that is depicted in Figure 5.5 to 5.7. After that the effect of precipitation or rainfall was checked for different slope profiles with different slope angles. For this analysis, SEEP/W was used to incorporate the different intensities of precipitation (i.e., max. rainfall, min. rainfall, and avg. rainfall). For the slope with slope angle  $29.36^\circ$ , the factor of safety at max. rainfall, min. rainfall and avg. rainfall came out to be 1.207, 1.362 and 1.178 respectively as depicted in Figure 5.8 to 5.10. Similarly, for the slope with slope angle  $37.65^\circ$  the factor of safety at max. rainfall, min. rainfall and avg. rainfall came out to be 0.992, 1.085 and 1.137 respectively as depicted in Figure 5.11 to 5.13. Likewise, for the slope with slope angle  $42^\circ$  the factor of safety at max. rainfall, min. rainfall and avg. rainfall came out to be 0.928, 1.011 and 1.015 respectively as depicted in Figure 5.14 to 5.16. The graph that has been plotted between shear resistance and shear mobilised before and after rainfall as shown in Figure 5.8 & Figure 5.18 shows how resisting forces and destabilising forces are playing their role in the slope stability. As in Figure 5.8 value of shear resistance is greater than that of shear mobilized value before rainfall which shows that the forces causing stability is greater than the forces causing instability which results in the stability of the slope, like this in Figure 5.18 value of shear resistance is lesser than the value of shear mobilized after rainfall which causes the

failure of the slope. This shows that the rainfall has a negative impact on the slope profile and causes instability of the slope. Figure 5.19 depicts the comparison between slope angle and factor of safety at different rainfall intensities (i.e., max. rainfall, min. rainfall, and avg. rainfall). This shows the effect of the intensity of rainfall combined with different slope profiles on the slope stability. The use of geosynthetics was incorporated for enhancing the slope stability. With the help of geosynthetics the slopes that were unstable after the impact of different intensities of rainfall and at different slope profile, they were made stable using the geosynthetics in different no. of layers which were 3, 4, 5 and 6 layers. The effect on stability of slope after using geosynthetics were depicted in Figure 5.20 to 5.27.

## CHAPTER 6 CONCLUSIONS

The district of Shimla is frequently impacted by landslides, that are considered as one of the environment's most hazardous and devastation risks. An investigation is done to examine the effect of percolation of rainfall into the different slope profiles with varying slope angle and their failure mechanism with the help of numerical modelling.

- The varied slope profiles were studied in order to see the effect of pre-monsoon and after rainfall effect on these profiles.
- The safety factor before pre-monsoon was found to be greater than 1 establishing a stable slope.
- The safety factor was less than 1 at the maximum rainfall for the slopes with slope angles of  $37.65^\circ$  and  $42^\circ$ , indicating an unstable slope.
- The failed slopes caused by precipitation were stabilised using geosynthetics in 3, 4, 5, and 6 layers.
- The factor of safety for the geosynthetic reinforced slopes after rainfall was greater than 1 indicating the stable slope.
- With the increase in the number of layers of geosynthetics, the safety factor of the slopes also increased.

The rainfall limit for an area can be determined using the results of this study. This study confirms the significant sensitivity of the Himachal Pradesh region to rainfall-induced landslides and identifies key slip surfaces that could be helpful for future mitigation strategies. The utility of numerical modelling for analysis in the Indian Himalayan regions was also confirmed by this study.

## REFERENCES

1. D. Bhattacharjee and B. V. Viswanadham, "Centrifuge model studies on performance of hybrid geosynthetic-reinforced slopes with poorly draining soil subjected to rainfall," *Journal of Geotechnical and Geoenvironmental Engineering*, vol. 145, no. 12, 2019.
2. T. R. Martha, N. Kerle, C. J. van Westen, V. Jetten, and K. Vinod Kumar, "Object-oriented analysis of multi-temporal panchromatic images for creation of historical landslide inventories," *ISPRS Journal of Photogrammetry and Remote Sensing*, vol. 67, pp. 105–119, 2012.
3. R. P. Gupta and B. C. Joshi, "Landslide hazard zoning using the GIS approach—a case study from the Ramganga catchment, Himalayas," *Engineering Geology*, vol. 28, no. 1–2, pp. 119–131, 1990.
4. C. Prakasam, R. Aravindh, V. S. Kanwar, and B. Nagarajan, "Landslide hazard mapping using geo-environmental parameters—a case study on Shimla Tehsil, Himachal Pradesh," *Lecture Notes in Civil Engineering*, pp. 123–139, 2019.
5. B. V. S. Viswanadham and D. Bhattacharjee, "Studies on the performance of geocomposite reinforced low-permeable slopes subjected to rainfall," *Japanese Geotechnical Society Special Publication*, vol. 2, no. 69, pp. 2362–2367, 2016.
6. Q. Zhai and H. Rahardjo, "Determination of soil-water characteristic curve variables," *Computers and Geotechnics*, vol. 42, pp. 37–43, 2012.
7. H. Rahardjo, T. H. Ong, R. B. Rezaur, and E. C. Leong, "Factors controlling instability of homogeneous soil slopes under rainfall," *Journal of Geotechnical and Geoenvironmental Engineering*, vol. 133, no. 12, pp. 1532–1543, 2007.
8. B. Krishnan and P. A. Vasantha, "Numerical modeling for the selection of coir geotextile for erosion control application based on the universal soil-loss equation," *Journal of Computing in Civil Engineering*, vol. 29, no. 6, 2015.
9. J. S. Dhanya, A. Boominathan, and S. Banerjee, "Performance of geo-base isolation system with Geogrid reinforcement," *International Journal of Geomechanics*, vol. 19, no. 7, 2019.
10. A. Mirzaalimohammadi, M. Ghazavi, S. H. Lajevardi, and M. Roustaei, "Experimental investigation on pullout behavior of Geosynthetics with varying dimension," *International Journal of Geomechanics*, vol. 21, no. 6, 2021. doi:10.1061/(asce)gm.1943-5622.0002051
11. S. Vadivel and C. S. Sennimalai, "Failure mechanism of long-runout landslide triggered by heavy rainfall in Achanakkal, Nilgiris, India," *Journal of Geotechnical and Geoenvironmental Engineering*, vol. 145, no. 9, 2019.



12. N. Tiwari, N. Satyam, and A. J. Puppala, "Effect of synthetic geotextile on stabilization of expansive subgrades: Experimental study," *Journal of Materials in Civil Engineering*, vol. 33, no. 10, 2021.
13. F. Bessa Ferreira, P. Pereira, C. Silva Vieira, and M. Lurdes Lopes, "Long-term tensile behavior of a high-strength geotextile after exposure to recycled construction and demolition materials," *Journal of Materials in Civil Engineering*, vol. 34, no. 5, 2022.
14. P. Ering and G. L. Babu, "Characterization of critical rainfall for slopes prone to rainfall-induced landslides," *Natural Hazards Review*, vol. 21, no. 3, 2020.
15. W. Tan, S. Qu, and D. Gao, "Stability analysis on highway slopes in Rainy Region," *Slope Stability and Earth Retaining Walls*, 2011.
16. R. Collins, M. Zhang, L. Hulse, and X. Zhang, "Stabilization of erodible slopes with Geofibers and nontraditional liquid additives," *Ground Improvement and Geosynthetics*, 2014.
17. H. Rahardjo, X. W. Li, D. G. Toll, and E. C. Leong, "The effect of antecedent rainfall on slope stability," *Unsaturated Soil Concepts and Their Application in Geotechnical Practice*, pp. 371–399, 2001.
18. H. Saito, D. Nakayama, and H. Matsuyama, "Relationship between the initiation of a shallow landslide and rainfall intensity—duration thresholds in Japan," *Geomorphology*, vol. 118, no. 1–2, pp. 167–175, 2010.
19. M. Sharma and R. Kumar, "GIS-based landslide Hazard zonation: A case study from the parwanoo area, lesser and Outer Himalaya, H.P., India," *Bulletin of Engineering Geology and the Environment*, vol. 67, no. 1, pp. 129–137, 2007.
20. P. Sharma, S. Rawat, and A. K. Gupta, "Study and remedy of Kotropi landslide in Himachal Pradesh, India," *Indian Geotechnical Journal*, vol. 49, no. 6, pp. 603–619, 2018.
21. S. Merat, L. Djerbal, and R. Bahar, "Numerical Analysis of climate effect on slope stability," *PanAm Unsaturated Soils 2017*, 2018.
22. P. Sharma, B. Mouli, R. S. Jakka, and V. A. Sawant, "Economical design of reinforced slope using geosynthetics," *Geotechnical and Geological Engineering*, vol. 38, no. 2, pp. 1631–1637, 2019.
23. S. Singh, "Effect of soil nailing on stability of slopes," *International Journal for Research in Applied Science and Engineering Technology*, vol. V, no. X, pp. 752–763, 2017.
24. R. Gupta, R. H. Swan, Jr., and J. G. Zornberg, "Laboratory pullout equipment for testing soil-geosynthetic interface for reinforced flexible pavement design," *Geo-Congress 2014 Technical Papers*, 2014.

25. B. Li, W. Yu, B. Gong, and Z. Cheng, "Centrifugal and numerical modeling of high and steep geosynthetic-reinforced slopes," *Geo-Congress 2013*, 2013.
26. S. V. Panikkar and V. Subramanyan, "A geomorphic evaluation of the landslides around Dehradun and Mussoorie, Uttar Pradesh, India," *Geomorphology*, vol. 15, no. 2, pp. 169–181, 1996.
27. A. P. Paswan and A. k. Shrivastava, "Modelling of rainfall-induced landslide: A threshold-based approach," *Arabian Journal of Geosciences*, vol. 15, no. 8, 2022.
28. GeoStudio (2005) *GeoStudio Tutorials include student edition lessons*, 1st edn. Geo-Slope International Ltd., Calgary.
29. Hammah, R.E., Yacoub, T.E., Corkum, B., and Curran, J.H., "A comparison of finite element slope stability analysis with conventional limit-equilibrium investigation." *Proceedings of the 58th Canadian Geotechnical and 6th Joint IAHC-CNC and CGS Groundwater Specialty: Saskatoon, Saskatchewan, Canada, 2005.*
30. D.G Fredlund, and H. Rahardjo, "Unsaturated soil mechanics," Wiley, New York, 1993.
31. A.P. Paswan and A.K. Shrivastava, "Stability Analysis of Rainfall induced landslides," *International Online Conference on Emerging Trends in Multi-Disciplinary Research, Rajasthan, India, 20-22 January 2022.* 505-509.
32. H. Rahardjo, A. Satyanaga, and E. C. Leong, "Unsaturated Soil Mechanics for Slope Stabilization," *Geotechnical Engineering Journal of the SEAGS & AGSSEA*, Vol. 43 No.1 March 2012, ISSN 0046-5828.

## LIST OF PUBLICATIONS

<b>S.No.</b>	<b>Paper Title</b>	<b>Category</b>	<b>Presented in</b>	<b>Publishing in</b>	<b>Status</b>
1.	Study of Rainfall Induced Landslide with Different Slope Profile	Journal	International Conference on Advances in Civil Engineering (ICACE)	AIP Conference Proceedings Journal	Accepted and in the process of publication
2.	Study of Slope Stability using Geosynthetics	Conference	5th International Conference on Recent Advancements in Engineering and Technology (ICRAET-2023)	Yet to be decided	Accepted in the conference

PAPER NAME

**Shubham (2k21GTE22) Thesis Library.do  
cx**

AUTHOR

**Shubham Singhal**

WORD COUNT

**9365 Words**

CHARACTER COUNT

**51112 Characters**

PAGE COUNT

**45 Pages**

FILE SIZE

**6.1MB**

SUBMISSION DATE

**May 24, 2023 11:50 AM GMT+5:30**

REPORT DATE

**May 24, 2023 11:50 AM GMT+5:30****● 12% Overall Similarity**

The combined total of all matches, including overlapping sources, for each database.

- 5% Internet database
- 6% Publications database
- Crossref database
- Crossref Posted Content database
- 9% Submitted Works database